Acta Biomaterialia xxx (xxxx) xxx

Contents lists available at ScienceDirect

Acta Biomaterialia

journal homepage: www.elsevier.com/locate/actbio

Review article

Graphene and graphene oxide for bio-sensing: General properties and the effects of graphene ripples

Gulsah Yildiz [a], Majbritt Bolton-Warberg [b,*], Firas Awaja [c,d,*]

[a] Department of Bioengineering, Konya Food and Agriculture University, Konya, Turkey
[b] National University of Ireland, Galway, Ireland
[c] Engmat Ltd., Clybaun Road, Galway, Ireland
[d] Department of Medicine, National University of Ireland, Galway, Ireland

ARTICLE INFO

Article history:
Received 10 March 2021
Revised 21 May 2021
Accepted 29 June 2021
Available online xxx

Keywords:
Graphene
Graphene oxide
Bio sensor
Ripples
Nano-indentation
Conductivity

ABSTRACT

The use of Graphene based materials, such as graphene oxide (GO), in biosensing applications is gaining significant interest, due to high signal output, with strong potential for high industrial growth rate. Graphene's excellent conduction and mechanical properties (such as toughness and elasticity) coupled with high reactivity to chemical molecules are some of its appealing properties. The presence of ripples on the surface (whether indigenous or induced) represents another property/variable that provide enormous potential if harnessed properly. In this article, we review the current knowledge regarding the use of graphene for biosensing. We discuss briefly the general topic of using graphene for biosensing applications with special emphasis on wearable graphene-based biosensors. The intrinsic ripples of graphene and their effect on graphene biosensing capabilities are thoroughly discussed. We dedicate a section also for the manipulation of intrinsic ripples. Then we review the use of Graphene oxide (GO) in biosensing and discuss the effect of ripples on its properties. We present a review of the current biosensor devices made out of GO for detection of different molecular targets. Finally, we present some thoughts for future perspectives and opportunities of this field.

Statement of significance

Biosensors are tools that detect the presence and amount of a chemical substance, such as pregnancy tests and glucose monitoring devices. They are general portable, have short response times and are sensitive, making them highly effective. Gold and silver are used in biosensors and more recently, graphene. Graphene is sheets of carbon atoms and is the only two-dimensional crystal in nature. It has unique features allowing its effective use in biosensing applications, including the presence of ripples (non-flat areas that give it its electronic properties). The last comprehensive review of this topic was published in 2016. This paper reviews the current knowledge of graphene based biosensors, with a focus on ripples and their effect on graphene biosensing capabilities.

1. Introduction

Biosensors are tools that detect the presence and amount of a chemical substance by combining physical and biological components [1]. Glucose monitoring devices and pregnancy tests are examples of very successful biosensors [2]. They are characteristically portable, have a short response time and are highly sensitive, making them important and effective tools. In addition, they are more efficient and cost-effective than current conventional detection methods such as polymerase chain reaction (PCR), and enzyme-linked immunosorbent assay (ELISA) [3,4].

There are number of materials being used in biosensor applications such as polymers [5], gold and silver [6], and recently, graphene. Graphene is a material comprised of two-dimensional sheets of carbon atoms packed in a hexagonal lattice. It is the only two-dimensional crystal in nature and gathering increased interest due to its unique electronic structures, transport and

* Corresponding authors:
E-mail addresses: gulsah.yildiz@ogr.gidatarim.edu.tr (G. Yildiz), majbritt.bolton-warberg@nuigalway.ie (M. Bolton-Warberg), Firas.awaja@nuigalway.ie (F. Awaja).

https://doi.org/10.1016/j.actbio.2021.06.047
1742-7061/

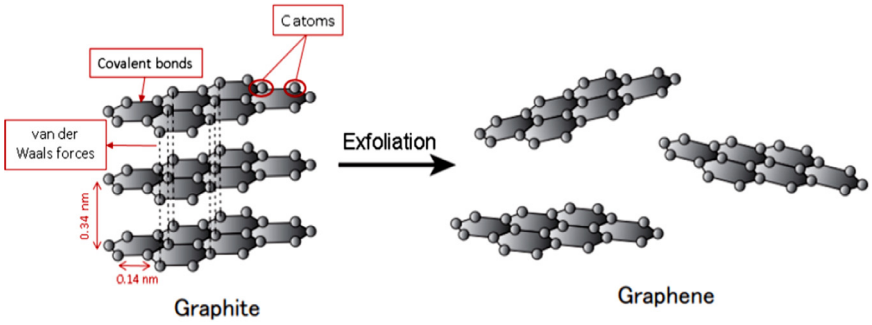

Fig. 1. Structure of graphite (layered) and graphene (monolayer) differences. Graphene is formed from the exfoliation of graphite. After the exfoliation process each platelets get separated from one another and form graphene sheets.

optical properties. Graphene contains non-flat areas called ripples, that disrupt graphene's flat surface and are responsible for its intrinsic electronic properties. These ripples, with an average size of 80 Å, are thought to be formed as a result of the bonding between the carbon atoms in graphene or thermal fluctuations [7]. Ripples can induce magnetic fields and alter local potentials of the graphene, resulting in changes in the electronic properties. In addition, local strain and band-gap of the graphene can be altered by adjusting the ripple formation, causing changes in the graphene properties [8]. As a result of these properties, graphene has become a significant material in biosensor applications and could open a new way to all-graphene-based electronic devices.

The aim of this article is to provide a comprehensive and critical review of the use of graphene (and its derivatives) as a biosensor. Furthermore, we discuss the effects of ripples on the functionality and performance of graphene materials- based biosensors. Although the topic of graphene biosensors has been reviewed previously, this review provides multiple novel discussions and updates the most recent review (2016) on the topic. Novel points of discussions include current challenges in biosensor applications and why graphene is a solution for these challenges. We describe the fundamental properties of graphene that promote accurate biosensing and ripples as an intrinsic property of graphene outlining possible advantageous and disadvantageous (structural, mechanical and molecular in addition to conductivity) for biosensing applications. We list current applications of graphene biosensors and explain the concepts behind detection mechanisms. Finally, we provide a perspective of the topic based on knowledge accumulated during the past decade and in particular the last 5 years.

2. Graphene

Graphene is a two-dimensional sp2 hybridized hexagonal crystalline material and is the monolayer form of graphite, which has a layered structure. Fig. 1 shows the graphite structure with its van der Waals forces which keep each graphene monolayer together and as graphite is exposed to exfoliation these forces break resulting in the formation of graphene sheets [9]. It is a widely used material with many applications such as sensors, structural composites, electronics, nanocomposites and supercapacitors, due to its enhanced chemical, mechanical and electrical properties [10]. The carbon atoms in graphene are prone to chemical reactions from all sides as a result of its monolayer structure and sp2 hybridised nature. This feature of graphene makes it a chemically active material that can be modified into desired structures [11]. Graphene has a very high tensile strength, making it very strong, but it is also lightweight and elastic [11].

Graphene is a highly conductive material, containing sp2 hybridized carbons in its structure (Fig. 2) [12]. Each carbon in the lattice is bonded together with (i) 3 σ bonds that are connected to other C atoms in the structure (Fig. 2a) and (ii) 2 π bonds that are

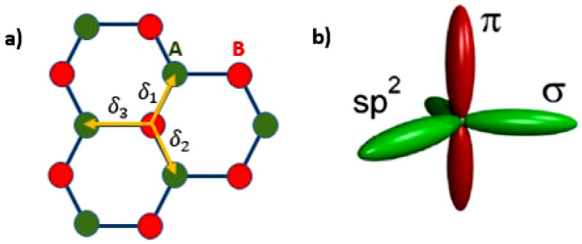

Fig. 2. (a) 3σ bonds (δ1, δ2 and δ3) in the structure of the sp2 hybridized graphene (Green dots represent A carbons and red dots represent B carbons). (b) 3σ bonds in-plane and 2 π bonds perpendicular to 3σ bonds in out-of plane [143].

perpendicular to the σ bonds (Fig. 2b). The π bonds are not connected to any other carbon and stand as free π electrons, which are mobile and can be delocalized through the graphene sheet. Therefore, because π electrons can move freely in the structure, graphene is a good conductor, having superior electrical properties and high carrier rate, reaching up to 15,000cm^2/V.s at room temperature [13].

In order for an electron to contribute to the conduction, there is a minimum energy required to excite that electron from valence to conduction band. This minimum energy is referred to as the bandgap [14]. Within metals, valence and conduction bands are touching so they have zero bandgap, meaning no energy is used in conduction. Graphene is also a zero bandgap material and it is sometimes called a zero-gap semiconductor or zero-gap metal [15].

Valence and conduction bands of graphene are cone-shaped and touch at 6 points, which are called Dirac points, representing the 6 vertices of the hexagonal lattice (Fig. 3a). These cones touch each other at K point (K and K′) which is located in the Brillouin zone (Fig. 3b,c) and they represent the Dirac points of the A and B carbons (Fig. 2) in a hexagonal lattice of graphene [6]. In the Brillouin zone, r is the center of the hexagonal shape, b1 and b2 are reciprocal lattice vectors [6], kx and ky are 2D wavevector components along the x and y directions, and M is the saddle point [16,17].

Valence and conduction bands touch in K and K′ at the Fermi level which is the energy at 0 Ev [18]. In addition, electron and hole masses are near zero at this point, which can be referred to as Dirac fermions [19]. Because electrons in graphene have zero mass, they move like a zero mass particle which makes them travel faster than any other conductor at room temperature. This electrical property makes graphene a great conductor [13].

2.1. Graphene for biosensing applications

Biosensors are being widely used for detecting chemical and biological substances in the human body, food industry and related

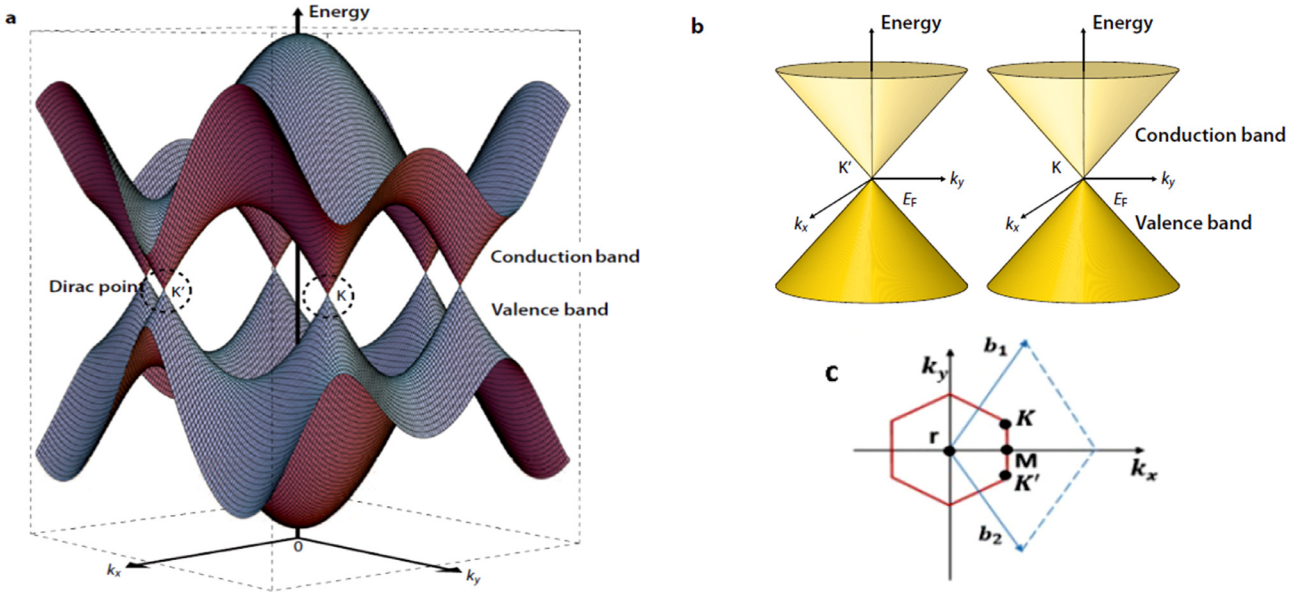

Fig. 3. Representation of the bandgap structure of graphene. (a) 3D representation of the Dirac points where valence and conduction bands touch at K and K′points [144]. (b) Intersection points of cone-shaped valence and conduction bands [144]. (c) The Brilliouin zone of graphene. Each lattice unit of the graphene contains the Brillioun zone that involves K and K'.

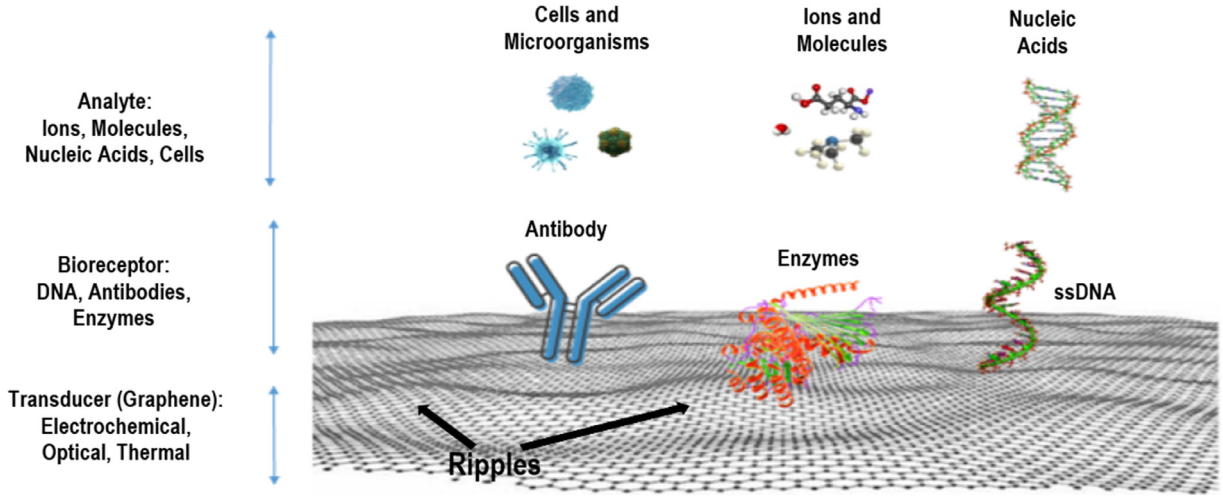

Fig. 4. Graphene is used as a transducer in different biosensors. A variety of bioreceptors, such as DNA, antibodies and enzymes, can be immobilized on graphene surface. This allows the graphene to detect a variety of analytes, such as ions, molecules, nucleic acids and cells.

areas. New nanomaterials are being utilized in order to increase the sensitivity and improve the efficiency of biosensors by capitalizing on their chemical and electrical properties [20]. Sensitivity, accuracy and having a low detection limit are all important characteristics in biosensor applications [21].

Graphene and graphene-based nanomaterials are one of the most important materials being used in nano-sensor applications as a result of their improved signal output [21]**.** Graphene is highly successful in detecting chemical and biological substances like DNA, bacteria, lipids, peptides, viruses, antibodies, and ions (Fig. 4) [22]**.**

A number of features make graphene an ideal material for use in biosensing applications including:

- Chemical flexibility of graphene materials which can also be improved with ripples and wrinkles. This increases the number of recognition or analyte elements that can be linked to the graphene surface. A high surface area increases sensitivity to chemical and biological substances [23]. Due to its monolayer structure and its sp2 hybridised nature, the carbon atoms in graphene can be modified with different functionalities, depending on the properties required for the biosensor in question. These modifications are easily made because graphene's π bonds create attraction sites and its monolayer structure enables molecules to get close to its surface [11]. For example, organic groups such as chromophores can be attached to the graphene surface and by perturbing the extended character of graphene, its electronic properties can be controlled [24].

Moreover graphene and graphene-based materials can immobilize different bioreceptors covalently or non-covalently, which make them excellent for biosensing applications. Single-stranded DNA can bind from its ring-structured nucleobases, to the graphene surface, by noncovalent interactions like π-π stacking, hydrogen bond and electrostatic interactions. Proteins can chemically attach to carboxylic groups of graphene oxide by their amine groups [25].

Table 1
Graphene based biosensors for detection of different targets. GOD: Glucose oxidase enzyme, Pt NPs: Platinum nanoparticles, ssDNA: Single-stranded DNA, Ag NPs: Silver nanoparticles.

Sensor Type	Target	Detection Method	Reference
Electrochemical	Glucose	Graphene/Nafion/Pt NPs/Chitosan/GOD	[33]
Electrochemical	Glucose	Graphene/GOD/chitosan	[34]
Electrochemical	Prostate Specific Antigen	Graphene sheet/Methylene blue/ Chitosan/Antibody	[35]
Electrochemical	Prostate Specific Antigen	Graphene sheet/Quantum dot functionalized graphene/antibody	[36]
Electrochemical	Pb(II)	Graphene field effect transistor/DNAzyme/Pyrene	[37]
Surface Plasmon Resonance	3-nitro-L-tyrosine	Graphene/Nickel	[38]
Surface Plasmon Resonance	Folic acid	Graphene	[39]
Surface Plasmon Resonance	ssDNA	Graphene/Gold nano urchin/ssDNA	[40]
Surface-enhanced Raman spectroscopy	Aristolochic acids	Graphene/Ag NPs/Fe3O4	[41]
Surface-enhanced Raman spectroscopy	Rhodamine B	N-doped graphene	[42]
Surface-enhanced Raman spectroscopy	Rhodamine 6 G/crystal violet/thiram	Graphene/Ag NPs/CuF	[43]
Optical	DNA	Graphene-MoS2/BK7 prism/Ag/SiO2/Au	[44]
Optical	Nitrate	Graphene/Optical fiber tip	[45]

- Electronic Properties due to its sp2 hybridized structure containing π bonds that are free to move on the graphene structure [23]. This high transfer rate of electrons allows a great sensitivity for electrochemical biosensors where electrons are moving between bioreceptor and graphene-made transducer [21].
- High Tensile Strength makes it stronger than diamond due to powerful C–C bonds. Moreover, Van der Waals forces increase its flexibility and make it a soft material. Being both strong but flexible at the same time is an important feature which makes graphene a widely used material in wearable-flexible biosensors [23].

A biosensor contains two main components: a bioreceptor, which identifies the analyte, and a transducer, that transforms the chemical signal produced by the bioreceptor into a measurable electrical signal [2]. Some examples of bioreceptors include aptamers, DNA, cells, and antibodies. Graphene is used as a transducer in biosensors. When an analyte interacts with the bioreceptor, a signal (heat, light or pH) is generated. In order to convert the chemical signal into a measurable electrical signal, bioreceptors should be linked to the surface of a transducer (e.g. graphene). Incorporation of graphene as transducers in biosensors increases electrical conductivity, rate of electron transfer and electrically active surface area to volume, which improves the sensitivity of the biosensors [26].

Graphene and graphene-based materials (e.g. Graphene Oxide(GO), reduced Graphene Oxide(rGO)) are primarily used in 5 biosensors: Electrochemical, Fluorescent, Optical, Surface plasmon resonance (SPR) and Surface-enhanced Raman Scattering (SERS) biosensors. Some examples of graphene based biosensors are given in Table 1.

Wearable graphene-based biosensors

The need for flexible biosensors is rapidly increasing in the medical field, the solution being to find materials that are flexible but still have high structural properties. Graphene is an ideal candidate due to its flexibility, high sensing features, high conductivity and transparent nature. Furthermore, its high surface area makes it suitable to immobilize desired bioreceptors and adjust sensor's sensitivity [27].

One of the examples of the application of a flexible-wearable graphene biosensor is the detection of lactate in the human body by Labroo et al. (2013). Lactate levels can be used as an indication of heart failure, drug toxicity, liver illnesses and metabolic disorders. It can be released with sweat and blood in the body. Current lactate detection methods are spectrophotometry [28], magnetic resonance spectroscopy [29], high-performance liquid chromatography [30], and amperometric biosensors [31]. These methods take time and have rigid properties so are not suitable for wearable or on-site applications. Labroo et al. (2013) first transferred a graphene electrode from a rigid substrate to a flexible substrate (polyester film) to construct the graphene lactate biosensor. They then immobilized the required enzyme for lactate which is lactate oxidase (LOD) onto the graphene surface [32].

After the implantation of the flexible biosensor in the human body, when lactate comes into contact with the sensor, lactate oxidase converts lactate and oxygen to pyruvate and hydrogen peroxide (H_2O_2) (Reaction 3). Then, H_2O_2 is oxidated on the graphene electrode and produces a current. This current is used to detect the lactate concentration in the body and as the concentration increases, the current response strengthens [32].

$$\mathbf{L-Lactate} + \mathbf{O_2} \overset{\mathbf{LOD}}{\rightarrow} \mathbf{Pyruvate} + \mathbf{H_2O_2} \quad (1)$$

Wearable biosensors can be affected by the mechanical stress and the sensitivity of the biosensor changes. Labroo et al. (2013) examined the change in the sensitivity and electrical conductivity of the graphene biosensor in response to a mechanical stress (e.g. bending). Results indicate that as bending angle and number increase, the response and conductivity of the graphene biosensor decreases (Fig. 5). They concluded that the highest response and conductivity occur when the graphene sensor is not bent. When the sensor contains an added 10 μM lactate and is bended with an angle of 45°, the current response decreases 64% and electrical conductivity decreases 30%. If the bending angle is increased to 180° , there are decreases of 81% and 76% in current response and electrical conductivity, respectively. The decrease in response was caused by the reduction in conductivity [32].

While bending the sensor decreases current response and electrical conductivity, it is still sensitive enough to detect low levels of lactate, making it a viable sensor [32].

3. Intrinsic ripples of graphene

3.1. Nature of intrinsic ripples

In general, graphene is widely considered a flat sheet material, however recent experiments have revealed that graphene contains wrinkles and, more importantly, "intrinsic ripples" in its structure [7].

These ripples can be formed if graphene contains defects or it experiences thermal fluctuations where C–C bonds in the structure are temporally and spatially modulated. Researchers at Radboud University carried out a simulation to find the nature of the ripples by observing the graphene ripples at room (300 K) and high (1000 K, 2000 K, and 3500 K) temperatures, concluding that intrinsic ripples can be formed in response to thermal fluctuations. This is a very promising finding because it indicates that ripples can be tailored artificially by altering the temperature [7].

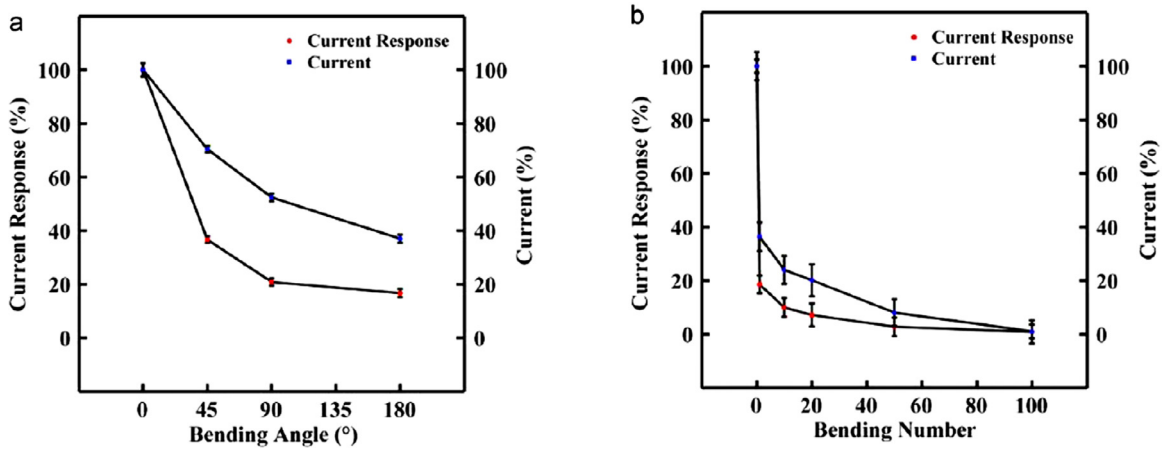

Fig. 5. (a) Relationship between bending angle of a biosensor and current response at lactate concentration of 10 μM. Current response decreases as bending angle increases. (b) Relationship between the number of times the biosensor is bent and current response. Current response decreases as bending number increases [32].

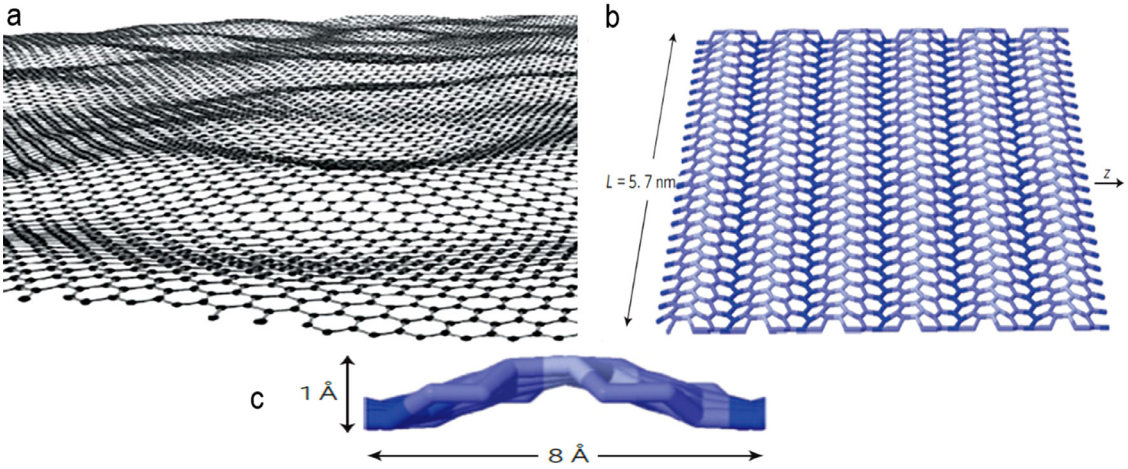

Fig. 6. Rippled graphene structure. (a) Image of a graphene with ripples. Ripples disrupt the flatness of the graphene and introduce out-of plane structures [46]. (b) Illustration of how ripples effect the structure of a graphene sheet, (c) Image of a single ripple with its amplitude and wavelength [145].

These modulations, like temperature or defects, lead C to occupy additional space in the 3rd dimension and ripples form. This change in the C causes electrons in the p-cloud to relocate and the symmetries of the bond lengths in the structure vary [46]. Disruption of the symmetry creates a non-planar structure and this non-planarity diminishes the free energy of the graphene. Thus, ripples conserve the stability of the graphene against the changes in its structure [47].

These long-wavelength fluctuations (ripples), with an amplitude of 1 Å, disrupt the order of two-dimensional crystals (Fig. 6) [11,46] . Ripple formation takes place mostly on the edges of the graphene and regions close to defects. When they form near defect areas, they release the stress in-plane, therefore, most of the time defects like grain boundaries and dislocations produce ripples on the graphene. [46]. It is also observed that under a compressive strain as the size of graphene sheet increases, wavelength and amplitude of the ripples increase as well [48].

Graphene contains two directions in its structure, called zigzag and armchair , names derived from the edge shape of the graphene stripe (Fig. 7a, [49]). Alignment of ripples through the hexagonal graphene lattice can be along these two directions with the majority produced along the zigzag direction (Fig. 7b, c). Under a compressive strain, ripples along the zigzag direction have a lower energy than ripples along the armchair direction, hence it is easier to produce ripples along the zigzag direction (Fig. 7d) [50]. Hexagonal graphene structure contains 3 zigzag axes, resulting in 3 preferable direction for ripples to be formed along [51].

3.2. Ripples effect on the graphene

Ripples have a strong influence on the properties of the graphene in that they disrupt the existing structure and introduce new features. As a result, they have a significant impact on the mechanical and electrical properties of the graphene [46].

3.2.1. Ripples effect on the mechanical properties of the graphene

Graphene has one of the highest tensile strength of all materials and a high Young's modulus, which is the relation between stress and strain [52], that gives graphene its great mechanical properties [53]. Ripples principally alter the structure of the graphene and introduce new mechanical properties by manipulating the strength, elasticity and bending properties of the graphene.

For example, ripples can affect Young's modulus of the graphene which gives the elongation or compression of a material when it is loaded with force [54]. Experimental work has revealed that when ripples are suppressed with a strain, Young's modulus of the graphene increases. Therefore, if graphene has ripples, Young's modulus is decreased and more force is required to modify the graphene structure [55].

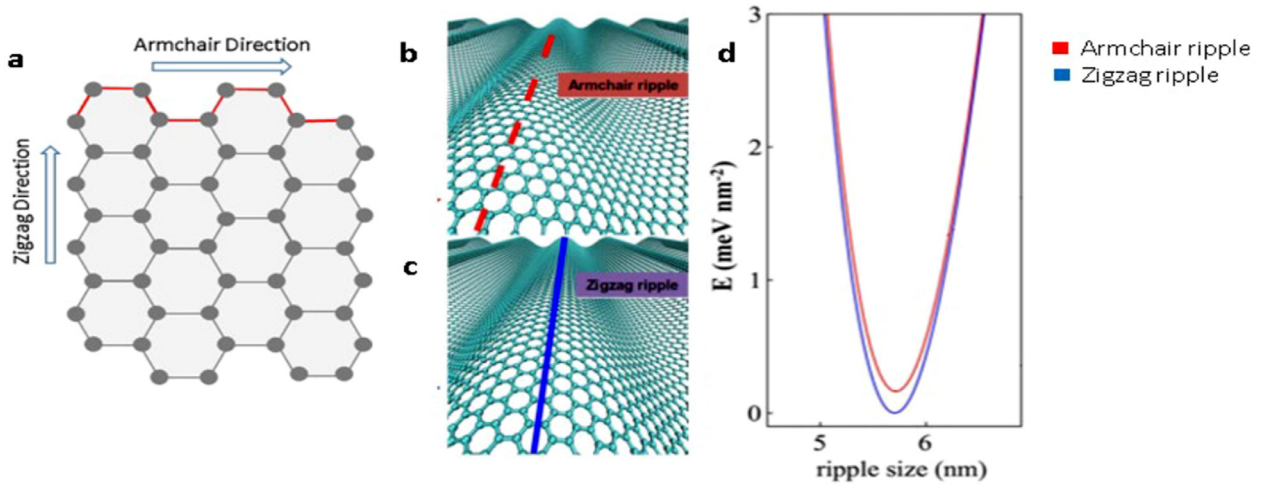

Fig. 7. (a) Armchair and zigzag structures through the hexagonal graphene [49]. (b,c) Armchair and zigzag alignment of the ripples through the hexagonal graphene. d) Relation between the energy and alignment of the ripples. As it can be seen from the graph alignment of ripples along the zigzag direction requires lower energy [50].

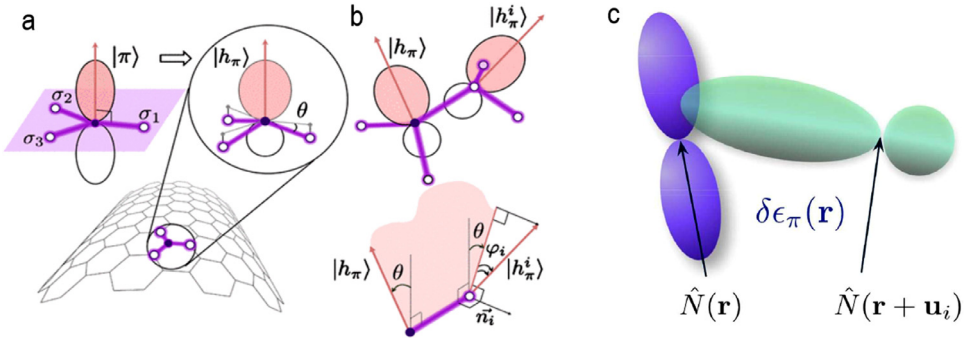

Fig. 8. Formation of the pyramid after bending (rippling). (a) Before bending, 3σ bonds are perpendicular to π orbital whereas the bending change the perpendicular structure and by introducing a "θ" angle a pyramid structure is formed in the orbitals of the carbon. (b) Pyramid structure is shown for two C atoms' orbitals [62]. (c) The re-hybridization between π-σ due to the bending which results in the change of the electrochemical potential [60].

Intrinsic ripples increase the elasticity of the graphene making graphene a suitable material for elastic bio-sensing applications [56]. However, as rippling of the graphene increases, its bending property decreases [57].

3.2.2. Ripples effect on the electrical structure of the graphene

In general, ripples introduce variable potential or magnetic fields to graphene [58]. They change the structure by manipulating the transport properties, band gap, bond structure and hybridization behaviours [59]. This is related to 3 main structural changes: (a) rotation of pZ orbitals, (b) re-hybridization between π and σ orbitals and (c) shortening of C–C bond length [60].

a) Rotation of pZ orbitals

When ripples are formed on the surface of the graphene, bending occurs in different amplitudes along the graphene surface (Fig. 8a,b) depending on environmental factors such as temperature and strain. This bending produces a rotation between pZ orbitals and the rotation diminishes the distance between the orbitals. As a result of the decrease in the distance, pZ orbitals' two lobes overlap more, eventually leading to re-hybridization between π and σ orbitals [61].

b) Re-hybridization between π and σ orbitals

Sp2 hybridized hexagonal graphene contains σ orbitals that are parallel and pZ orbitals that are perpendicular to the structure of the graphene sheet. When sp2 hybrids overlap each other because of the rotation of pZ orbitals, strong bonds of the structure are formed which causes stiffness in the graphene. pZ orbitals, on the other hand, contribute to the weak bonds of the structure. However, when ripples produce bending of the structure, it causes carbons and their neighbours to form a pyramid where each carbon becomes the corner, and the planar shape of the structure is no longer present (Fig. 8a,b) ([62]. The re-hybridization occurs when π orbital couples with three σ bonds and antibonds and with 3 s orbitals at three neighbours (Fig. 8c) ([61].

This re-hybridization causes charge impurities in the structure and electronic levels to shift, leading to a charge transport between valence and conduction levels. As a result of this transport, some energy levels become empty while some become occupied resulting in the formation of electron and hole puddles in the structure [46]. Charge impurities in the structure cause electron scattering. Electrons do not travel straight through different paths freely anymore but because of the charge impurities in the structure they scatter [63]. This scattering caused by ripples leads to electrical resistance and decreases the conductivity [64].

c) Shortening of C–C bond length

Ripple formation is also linked to decreases in the C–C bond [60]. When graphene is in its ground state, all bonds are in equivalent. However, a change in the orbitals and the formation of electron-hole puddles can alter the length between bonds. As temperature increases and becomes T = 300 K, bond lengths in the structure begin to vary. If bonds with different lengths occur in the same graphene structure, the planarity of the membrane becomes disrupted and ripples formation takes place [7].

Ripples introduce a band gap to the graphene

Graphene is known as a zero-gap material, meaning it is a very good conductor but there is no way of controlling this conductivity.

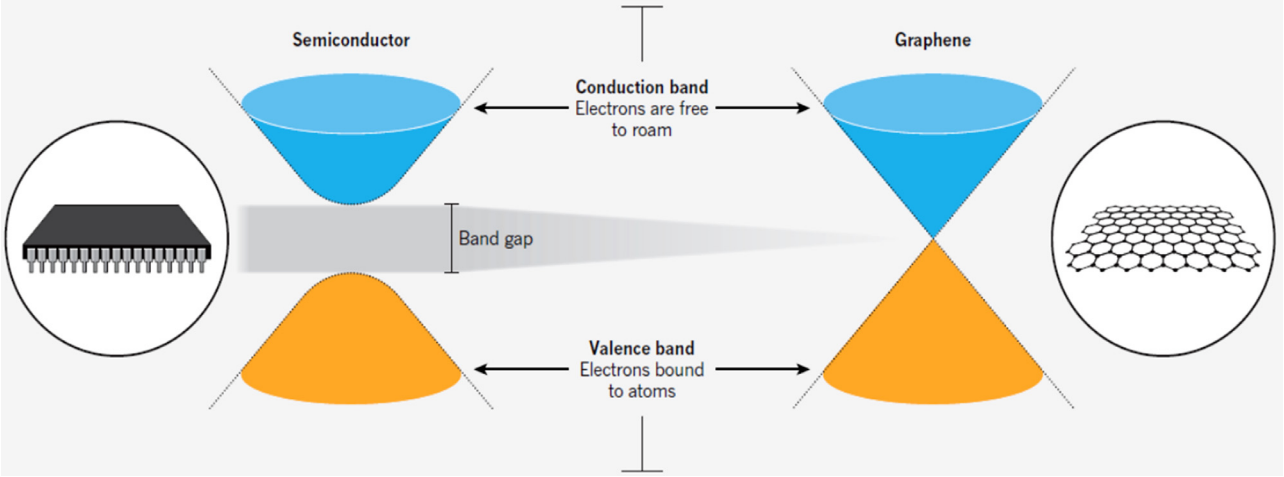

Fig. 9. Band gap difference between graphene and semiconductor. Semiconductor has a band gap between the valence and conduction bands. However, Graphene does not have any band gap, valence and conduction bands are touching [65].

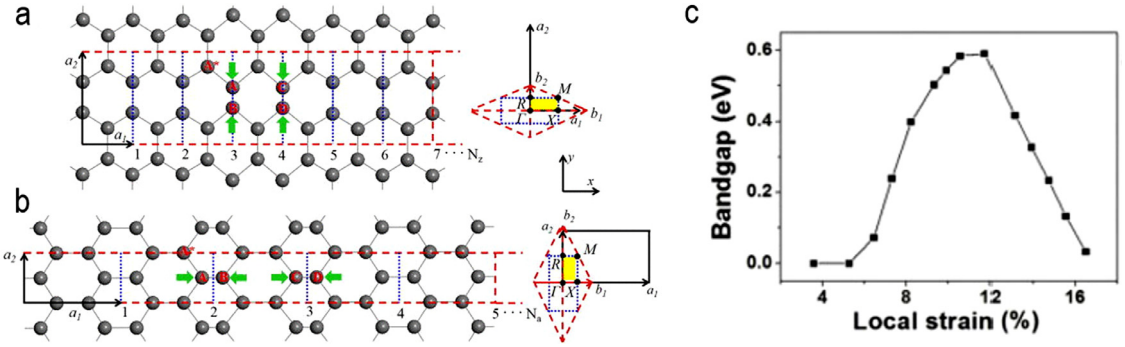

Fig. 10. (a) Compressive strain along zigzag direction and (b) along armchair direction (Gui et al., 2015). (c) Change in the band gap of a graphene structure under four atom local strain along zigzag direction [66].

The presence of a band gap in graphene is thus very important in digital electronics, because it introduces a way of controlling the conductivity which is not possible with zero-gap materials. [58].

In a zero-gap structure, valence and conduction bands are touching. In order to open a band gap and turn graphene into a semiconductor, distance between valence and conduction band should be more than zero (Fig. 9) [65]. The zero band gap of graphene comes from its symmetry between two types of nonequivalent carbon atoms (A and B carbons in Fig. 2). In order to open a band gap, this symmetry must be broken which can be achieved using multiple methods including growing it on different substrates (e.g. metals), applying a force, hydrogenating it in a certain pattern or cutting it in nanoribbons [18].

Band gap can be increased with different methods such as oxygenation or nanoribbons but they can have adverse effects on the electronic properties of graphene. Therefore, the most widely used method to increase the band gap without any adverse effect is to apply strain and to produce ripples [66]. So, it can be stated that the most important change that ripples provide is to introduce a band gap to the zero-gap graphene [67].

The previous structural changes which are rotation of pZ orbitals, re-hybridization between π and σ orbitals and shortening of C–C bond length can open a band gap in the graphene. As ripple amplitude increases, the distance between the valence and conduction bands increases [58] and the band gap of the graphene proportionally increases [68].

In order to produce ripples, compressive strain can be applied along the zigzag or armchair directions (Fig. 10a,b). Experiments show that armchair direction cannot open a significant band gap in the graphene, therefore only strain along the zigzag direction is considered here. When a compressive strain is applied to the graphene along zigzag direction, C–C bonds are squeezed and a band gap is initiated. When a band gap is opened, graphene is converted from a metal to semiconductor form. If strain is increased beyond a certain point, the graphene begins to deform and the band gap decreases or returns to zero, resulting in the graphene returning to its metal form (Fig. 10c). [66].

Graphene can also be stretched to adjust the band gap using methods other than applying compressive strain. When the graphene is stretched along the zigzag direction, the lattice structure of the hexagonal graphene collapses (Fig. 11). Since lattice structure is disrupted, ripples appear along the direction perpendicular to the stretching and the band gap opens as a result [69].

Consequently, the intrinsic ripples of graphene have been drawing a lot of attention owing to their characteristics mentioned above. Therefore, exploring the nature of the intrinsic ripples is important because it can open a new way to understand the electronic properties of graphene and to adjust them [7].

3.3. Ripples effect on graphene biosensing capabilities

Since ripples affect the chemical, mechanical and electrical properties of graphene, this has implications for any biosensors made from graphene, in particular the sensitivity of the sensor.

3.3.1. Flexibility

For use as non-flexible biosensors, graphene can be placed on a flexible substrate such as Polyethylene terephthalate (PET) or Poly-

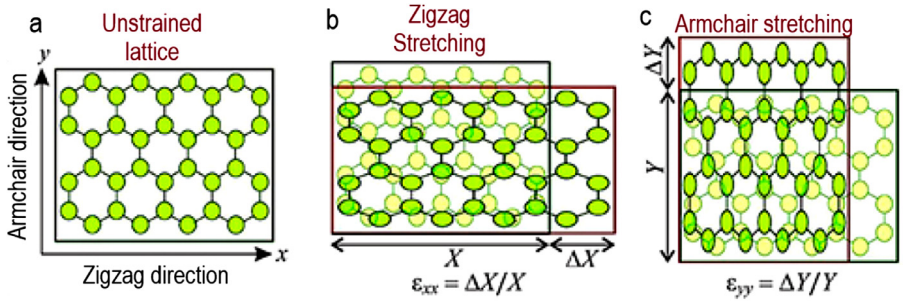

Fig. 11. Graphene (a) hexagonal structure without any stretching, (b) hexagonal structure under zigzag stretching, and (c)hexagonal structure under armchair stretching [69].

dimethylsiloxane (PDMS) with van der Waals interactions. Wearable biosensors, on the other hand, require a flexible graphene sheet. Flat graphene sheets can only be stretched up to a certain point (~6% strain), beyond which they get damaged under the strain, rendering them non-applicable for wearable biosensors [70]. This problem can be solved by introducing ripples to the graphene sheet, which produce out-of plane deformations, increasing the stretchability of the sensor [71]. Ripples on the graphene sheet unfold and allow the stress to be relieved as strain is applied to the graphene sensor. As a result of these out-of-plane structures, flexible electrodes can be stretched up to almost 400%, allowing sensors to maintain their conductivity by preventing break formation [72].

In an experiment conducted by Lai et al. (2014), flexible transistors were produced that can be stretched up to 50% [73] by combining graphene with PMMA-poly (3- butylthiophene). Moreover, these ripples give stability to the graphene sheet against stretching which makes it a highly suitable material for wearable sensors[74].

3.3.2. Increase in surface area

Another advantage of ripples on graphene is the increased surface area of the electrode [75]. This large surface area on graphene provides a region for successful immobilization of bioreceptors [76]. As an example, Hui et al. (2013) produced a biosensor for glucose detection, by immobilizing glucose oxidase enzyme (GOD) on a graphene sheet which was also covered by nafion film. The final product resulted in a high stability and high electron transfer rate between GOD and the graphene electrode surface. They reported a sensitivity of 21.9 $\mu A\ mM^{-1}cm^{-2}$ for glucose concentrations between 2 and 14 nM. Moreover, they observed that the graphene sheet contained crumples and wrinkles which had a similar structure to ripples and indicated that these structures enhanced the immobilization area for GOD [77].

In another study, Perumal et al. (2018) produced a biosensor that detects tuberculosis, which is a chronic and infectious disease. Gold nanoparticles were combined with a 3D graphene sheet to improve the sensitivity and selectivity of the biosensor. The graphene sheet had a rippled structure with self-assembled gold nanoparticles located on these rippled paths that produced rod-like formations. These formations provided a large and active surface area, resulting in increased immobilization rate of the sensor and improved hybridization efficiency [78].

Consequently, it can be concluded that ripples provide a high electroactive surface area for electrodes in biosensing applications [79].

3.3.3. Conductivity

Ripples affect the electrical structure of graphene by producing charge impurities in the structure so that electrons cannot travel through the graphene freely. This impact introduces electrical resistance to the graphene and the conductivity rate decreases [63,64].

As mentioned earlier, electrical conductivity of graphene is important in biosensor applications since high conductivity of graphene facilitates high transfer of electrons between the transducer and bioreceptor, resulting in high sensitivity of electrochemical biosensors [80]. It is thus expected that ripples decrease sensitivity and ultimately the efficiency of biosensors, despite the presence of ripples and wrinkles in almost all graphene-based biosensors. When constructing a graphene biosensor, it is important to consider the advantages (increased surface area) and disadvantages (decreased electrical conductivity) of ripples.

Ripples and wrinkles improve the properties of wearable flexible biosensors which are significant in real-time and consistent sensor applications. Since they are inserted into the human body, these wearable sensors must maintain both flexibility and electrical conductivity when a strain is applied. In order to provide these features, electrodes with specific materials should be produced which can be stretched but not lose their conductivity under a large strain [81].

Chiang et al. [70] produced a stretchable and sensitive photodetector based on hybrid graphene and graphene quantum dots. Pre-strained (25%) rippled Poly(dimethylsiloxane) (PDMS) was used to support a rippled graphene sheet and as a result a stretchable biosensor was obtained. Chiang et al. [70] conducted trials to see the effects of applied strain on the resultant conductivity of the biosensor, observing that as strain is applied, graphene conductivity increased up to a maximum level at 25% strain, beyond which conductivity decreases due to over strain (Fig. 12a). Applied strain decreases the amplitude of ripples on the graphene surface which allows electrons to move freely on the structure. Sensor structure under 0% strain and 25% strain is shown in Figs. 12b & c. Theoretically, it had been estimated that conductivity would increase non-stop as strain is applied. However, this study showed that beyond pre-strain level, the graphene structure becomes disrupted and conductivity diminishes [70].

In a similar trial, Wang et al. [71] combined rippled graphene with PDMS (prepared with 20% pre-strain), producing a rippled electrode. They subjected the electrode to varying levels of strain to study the strain-conductivity relationship. At 0% strain, device resistance was 5.9 kΩ, decreasing to 3.6 kΩ (relaxed graphene state-flat graphene) under a 20% strain. Reduction in resistance corresponded to an increase in electrical conductivity enhancement in sensitivity [71].

3.3.4. Ripples effect on biomolecules

Ripples on the graphene surface are defect formations and they are chemically more reactive than non-defected regions. Improved reactivity of ripples affects the bioconjugation ability of the graphene. So conjugation of biomolecules on graphene

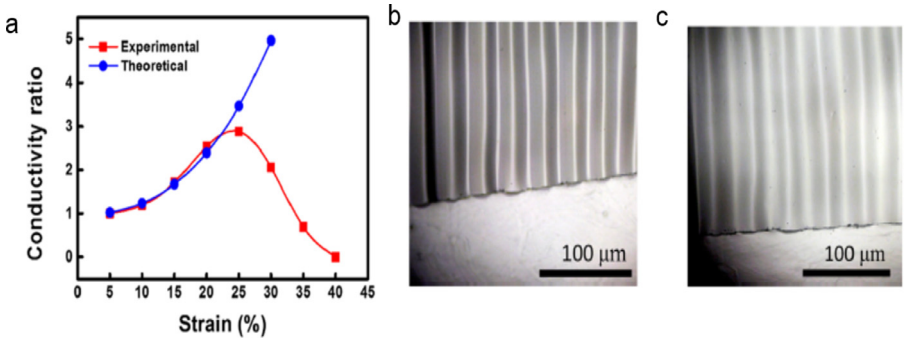

Fig. 12. Sensor structure (a) under 0% strain, (b) under 25% strain [70]. (c) The strain and conductivity relation. Theoretical estimation of conductivity is to increase as strain is applied. However, it is detected that conductivity of the sensor increases up to pre-strain level (25%) then it starts to fall down [70].

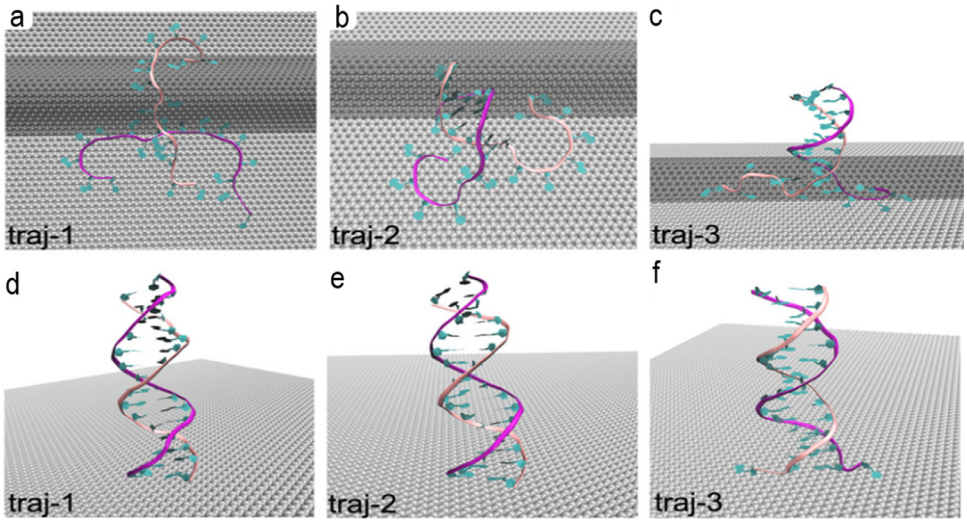

Fig. 13. (a-c) The native helical structures of dsDNAs change after interaction with W-Gras. (d-f) The native helical structures of dsDNAs remain the same after interaction with I-Gras [84].

substrate can be altered by modifying the ripples on the surface [82].

Ripples can also induce formation of a rough surface on the graphene sheet. As the surface roughness increases these areas (ripples, wrinkles) become anchorage sites for cells and biomolecules that enhances the adherence to the substrate surface. Increase in adherence directly improves the sensitivity of the graphene biosensors [83].

Moreover, ripples may also induce some adverse effects during graphene biosensing applications such as denaturating the structure of the analyte molecule. Li et al. (2020) carried out simulations of double stranded DNA (dsDNA) with both wrinkled graphene (W-Gra) and idealized graphene (I-Gra). They observed deformation in the helical structure of dsDNA when it interacted with W-Gra. When dsDNA interacted with I-Gra, the structure of dsDNA did not change, remaining stable. One possible reason for this difference is the binding energy of dsDNA, which is higher for W-Gra than I-Gra, which makes dsDNA strongly attracted to the wrinkled area and the terminal bases act as anchors. When other parts move but the terminal bases are anchored, the hydrogen bonds of the dsDNA break and the native structure of the dsDNA is deformed (Fig. 13). Wrinkles and ripples have similar structures, therefore the effects of wrinkled graphene here can be extrapolated for rippled graphene effect on dsDNA structure in biosensor applications. In addition, Li et al. (2020) reported that the effects of wrinkles in biomolecules are not fully understood and could potentially have undesired effects when working with biomolecules [84]. These findings should be considered while working with graphene-based biosensors.

3.3.5. Reactivity

Ripples cause curvature formations on the surface of the graphene and these curves possess higher charge density than planar regions [85]. Since charge density is directly related to the reactivity, ripples modify the local reactivity on graphene surface. For instance, Kowalik et al. observed that single copper atom's binding to rippled regions is 20 kcal/mol energetically more stable than binding to plane regions. So, it states that copper atoms prefer to bind rippled sites than planar areas of graphene. It can be caused since rippled sites have higher charge density than other regions so that mostly atoms prefer binding these sites. This property can be effectively used for graphene biosensor applications. By adjusting the ripples on the graphene surface, different molecules' affinities to substrate can be modified so that sensitivity of graphene based biosensors can be increased [86].

4. Manipulation of intrinsic ripples

Because ripples have a huge impact on the properties of graphene, their manipulation is important to control the graphene-based-electronics and to provide the desired features. There are several methods used to manipulate graphene ripples including thermal manipulation, strain-based manipulation, nano-indentation and vacuum annealing [8].

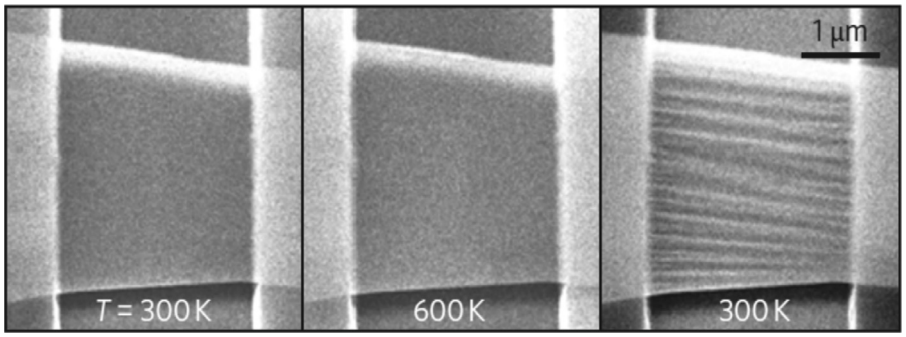

Fig. 14. Dependence of ripple morphology on temperature. When T is raised to ~600 K, the graphene sheet is flat, and any pre-existing ripples almost completely disappear. However, after cooling down to 300 K, ripples invariably appear, usually with much larger amplitudes than any previous ones [8].

4.1. Thermal manipulation

Thermal manipulation of intrinsic ripples is the most widely and usually the most effective method used to change the properties of the ripples.

The coefficient of thermal expansion (CET) describes how the size of an object varies with a change in temperature [87]. Graphene can obtain both negative and positive thermal expansion coefficients. The temperature ranges reported for negative CTE varies between different experimental studies. For instance, Gao et al. (2014) detected negative CTE at temperatures between 30 and 300 K [88], while another study estimated the range between 0 and 500 K [89]. Thus, the negative CTE range of graphene is not exact and can have varying values. When a graphene sheet is subjected to a temperature between the negative CTE values, and, the temperature increases, the graphene shrinks and ripples form on the membrane. In contrast, when temperature decreases within these negative CTE values, graphene expands and the sheet becomes almost perfectly flat and intrinsic ripples on the surface disappear [88].

However, graphene can also possess positive CTE. Gao et al. (2014) reported 300 K as the transition temperature from negative to positive CTE. When temperature is increased to values higher than 300 K, graphene possesses positive CTE. In another study, a transition value of 500 K was reported [89]. When temperatures rise above the transition value, graphene expands, and ripples disappear on the membrane. Conversely, when the temperature decreases, graphene shrinks, and ripples form on the graphene surface (Fig. 14) [88].

Therefore, elasticity is correlated with the rippling effect and by adjusting the temperature, elasticity of the graphene can be modified [8]. Moreover, because graphene has a very low thermal expansion coefficient, devices made from graphene will not show adverse effects due to temperature change, an important property [58].

4.2. Strain-based manipulation

The second manipulation method used to introduce intrinsic ripples is application of strain to the graphene sheet. As strain applied to the graphene increases, the amplitude of the ripples decreases. In addition, ripples have a very low amplitude (almost disappear) in the direction of strain and move perpendicular to the direction of the strain. This outcome is referred to as uniaxial strain (Fig. 15). When strain is applied biaxially, ripples can almost disappear in two directions and the graphene sheet will become almost ripple-free. However, as ripples disappear, the elasticity of the graphene will also decrease and it will become more rigid [56].

4.3. Nano-indentation

The third manipulation method is called the nano-indentation technique which involves the formation of cavities. In this method, Atomic Force Microscopy (AFM) is used to produce new periodic ripples on the graphene structure. AFM contains a probe in its tip and applies a mechanical load onto a desired site of the graphene sheet up to 600nN and after removing the load, ripple formation is observed on the site (Fig. 16a-c). Applying a load with AFM on the graphene produces ripples, 15 nm in amplitude, on the surface and consequently, the structure in Fig. 16c is generated. These images were also generated by AFM [90].

By implementing this method, ripples can be produced throughout the graphene sheet in desired size, shape and number. However, limitations were observed in the experiments, with several indentations at the same spot on the sheet resulting in no change the morphology of the ripple [90].

4.4. Vacuum annealing

The final method we will discuss that causes manipulation of ripples is called vacuum annealing. Principally, it is not used as a direct manipulation technique but rippling is affected after its application.

Graphene films are obtained using different techniques such as micromechanical exfoliation where a graphene sheet is formed by cleaving the graphite or it can be synthesized from chemical vapor deposition using volatile precursors [87–91]. Following synthesis the sheets are sometimes manipulated using different techniques such as thermal or strain-based methods to produce ripples. These processes can introduce contaminations to the graphene sheets which impacts their electrical properties. To reduce contamination, several cleaning procedures are applied to the graphene and one of the widely used methods is vacuum annealing [92].

For the annealing process, a graphene sample is put in a chamber at a specific temperature in a vacuum and subsequently cooled down to room temperature. [90]. The annealing process can result in two different kinds of graphene structures. Annealing at low temperatures reduces ripples and defects, whereas annealing at high temperatures causes structural disorder in the graphene sheet and produces ripples [93].

5. Graphene oxide

Graphene oxide (GO) is a material that is similar to graphene but it contains oxygen based-functional groups in its structure (Fig. 17, [94]. In fact, as these functional groups are removed, graphene oxide can almost be converted into graphene.

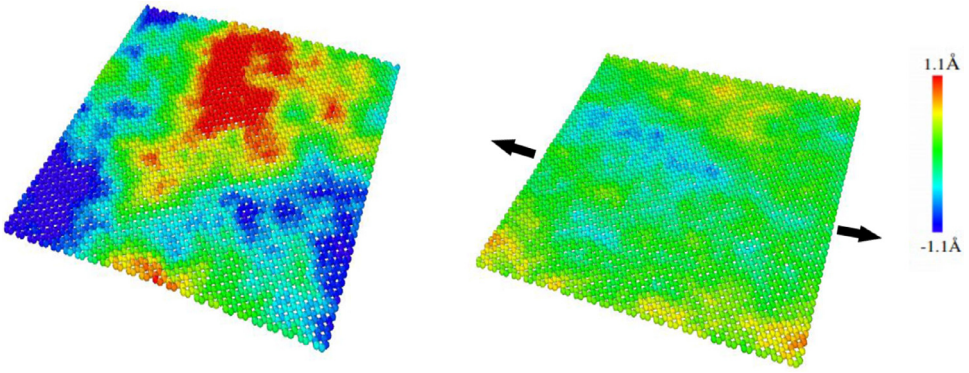

Fig. 15. Simulations showing the out-of-plane fluctuation of a monolayer graphene at 300 K with (a) 0% strain and (b) 0.5% strain. Green regions show where amplitude of ripples decreased tremendously [56].

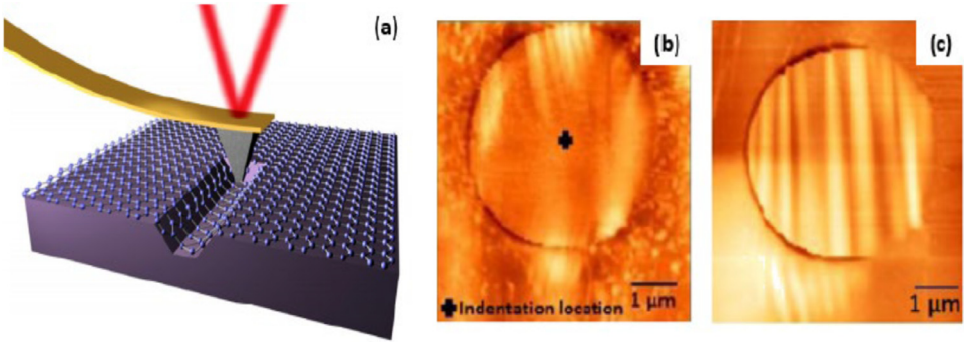

Fig. 16. (a) Atomic force microscopy introduces strain in graphene locally [146]. (b-c) Before and after image of nano-indentation to graphene. Before applying load with AFM there is no observable ripple on the graphene surface. However, after applying load with AFM into the same area, there are many observable ripples on the surface[90] .

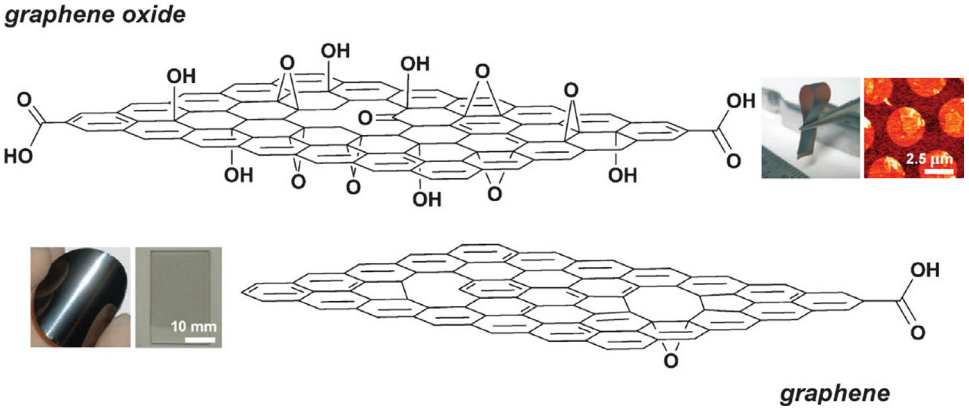

Fig. 17. Structural differences between graphene oxide (top) and graphene (bottom). Minimal oxidation (-O and -OH groups) visible in graphene compared to graphene oxide. [95].

Synthesis of graphene oxide is mostly undertaken through the oxidation of graphite, which is a multilayer form of graphene. This oxidation process produces graphite oxide by disrupting the crystalline structure of the graphite, introducing new wrinkles and increasing the length between adjacent sheets [95]. Then, graphite oxide multilayers are separated and monolayer graphene oxides (GO) are formed [96].

Oxidation of the graphene (with –O and -OH) increases the bond length between C–C and results in a reduction of the tensile strength and elasticity of the graphene oxide. Moreover, as oxidation level increases, the structure of the graphene oxide converts from brittle to ductile [97]. Brittle materials break easily even without a large deformation. On the other hand, ductile materials can deform largely under a load until they break [98].

Graphene oxide has unique attractive mechanical, electrical and thermal properties compared to graphene. From a mechanical point of view, GO can be used as polymer nanocomposites due to its high tensile strength. For example, the tensile strength of a material made from GO and Polyvinyl alcohol (PVA) mixed, is five times higher than pure PVA-based materials. This is due to the strength of GO and the high number of oxygen functionalities in the GO and their interaction with the –OH groups in the PVA. This interaction results in significant hydrogen bonding and increases the strength of the end material [99].

From an electrical point of view, GO is not electrically conductive and is, indeed, used as an electrically resistive material. During synthesis of GO, the sp2 crystalline structure of graphene is disrupted, inhibiting the electron mobility of the material and

GO becomes a non-conductive material [99]. As a result of its low electrical conductivity, GO is primarily combined with other highly conductive materials to improve this property in electrochemical biosensor applications.

From a thermal point of view, GO possesses low thermal conductivity, unlike graphene. As a result, GO can be used as a thermal insulator in clothing, building insulation and flame retardants [99]. In addition, in thermoelectric instruments, low thermal conductivity improves the efficiency of thermal conversion [100].

5.1. Graphene oxide based biosensors

Graphene oxide (GO) is being widely used in a variety of biosensor applications [101]. It contains both hydrophobic sp2 and sp3 structures and hydrophilic oxygen functionalities on its base such as carboxyl, epoxy, hydroxyl and carbonyl groups. These oxygen functional groups give graphene oxide different properties to graphene sheets [102]. However, GO also has properties such as electrical, thermal, and mechanical properties, in addition to its stretchable, transparent, biocompatible nature and large surface area [103].

The most distinctive feature of GO is its oxygen functional groups which gives it a hydrophilic nature. This hydrophilic nature gives GO its biocompatibility [103], an ability to interact with water [104], prevents adhesion of microorganism and inhibits biofouling [105]. Moreover, these oxygen functional groups provide areas to attach different nanoparticles such as metal oxides, quantum dots (QDs) and semiconducting nanoparticles and improve the sensitivity of the biosensors [106].

Oxygen containing groups improve GO's affinity for aromatic rings and make it highly diffusible in water which are extremely important properties in biosensors [107]**.** These groups also a) provide sites to immobilize bioreceptors by $\pi - \pi$ stacking or H bonding to detect biomolecules [25] and b)give fluorescence quenching ability to GO which is an important feature in fluorescence biosensors where energy is transferred from an excited state of the dye to GO [108–110]. Fluorescence quenching in GO biosensors takes place when fluorophores (fluorescent chemical compound) are close to the sensor. Fluorophores typically emit photons, but in close proximity to GO they prefer to transfer their energy to the GO sheet [111]. Thus the fluorescence light emission of the dye-labelled probe stops until it leaves the GO sheet which makes it a great way to detect biomolecules in fluorescence biosensors. Overall, graphene oxide is a promising biosensor material that is widely used especially in electrochemical, fluorescent, optical, surface plasmon resonance and surface-enhanced raman scattering biosensors. Some examples of graphene oxide based biosensors are given in Table 2.

6. Ripples of the graphene oxide

Rippling effect presents in graphene oxide similar to graphene. However, as it is mentioned, graphene oxide differs from graphene by its oxygen functionalities and they improve the rippling effect.

As the degree of oxidation increases in the graphene oxide, the amplitude of the ripples on the surface also increases linearly (Fig. 18). In addition, it was experimentally observed that the amplitude of "oxidation-induced ripples of graphene oxide" is larger than "thermally-induced ripples of graphene"[132].

There is a ratio related to the rippling effect of graphene oxide called the Poisson's ratio. When a strain is applied to a material in y-direction, another strain is produced in the x-direction as response [133]. The Poisson's ratio is calculated by dividing the produced strain laterally to applied strain longitudinally and this ratio can be negative or positive. If the ratio is positive, when the material is stretched in x-direction, it becomes compressed in y-direction, in response. If the ratio is negative, when the material is stretched in x-direction, it also becomes stretched in y direction, in response (Fig. 19) [132].

It was also observed that ripples of the graphene oxide have an impact on its physical and mechanical properties. Particularly, ripples of the graphene oxide decrease the value of Young's modulus of GO. As mentioned previously, Young's modulus is a property that gives the elongation or compression of a material when it is loaded with force [54]. Thus more force is needed to create a specific impact on the GO [132].

Based on experimental studies, rippling can induce Negative Poisson's Ratio (NPR) in the graphene, since the ripples will almost disappear when the graphene is stretched. As a result, it is assumed that rippling can also affect Poisson's ratio of GO and can lead to NPR. When oxidation degree is high ($p = 0.6125$), meaning GO has NPR, if GO is stretched in x-direction, y-direction of GO is also stretched and the amplitudes of the ripples decrease in all directions (Fig. 20, [132]).

In summary, as the degree of oxidation in GO increases, ripple formation and ripple amplitude also increases in GO. As a result, the Poisson's ratio decreases and can even become negative (Fig. 21).

6.1. Ripples effect on graphene oxide biosensing

The effect of ripples on the properties of graphene oxide can also be seen in biosensors made from GO. Ripples change the properties of GO such as flexibility, surface area, conductivity, and fluorescence quenching ability.

6.1.1. Flexibility

Ripples increase the flexibility of graphene oxide similar to their effect in graphene. Electrode materials used in wearable biosensors should be flexible and this can be achieved by introducing ripples to them. Since graphene oxide can contain ripples in its structure, it is an ideal candidate for use as an electrode material [134]**.** Tang et al. (2017) reported that ripples/wrinkles play a role in the stabilization of graphene and hypothesized that these structures also provide flexibility to graphene oxide sheets**.**

6.1.2. Surface area

The surface area of graphene oxide increases with the number of ripples on the surface [135]. This increase in surface area provides more sites to immobilize bioreceptors for biomolecule detection which improves the sensitivity of GO-based biosensors [76]. Moreover, an increase in surface area of GO provides more sites to immobilize conductive materials like gold nanoparticles [136], Fe3O4 nanoparticles [137]. As an example, Liu et al. (2010) produced a fluorescence biosensor based on GO and they immobilized Au NPs on the surface of GO, particularly to the wrinkled areas and folded edges. Thus, ripples can be used as primary sites for nanoparticle immobilization [112]. Ripples not only increase the surface area, they also provide a rough surface to graphene oxide which is ideal for loading different materials on GO such as quantum dots, nanoparticles etc. [138].

Ripples can also improve the efficiency of photodetectors. For example, the rough surface area that ripples and wrinkles provide improves the photoabsorption properties of the detector [138]. In another study, with ripple-like structures in photovoltaic devices with an organic semiconductor, it was observed that light absorption of the device increased. Light absorption improved from 4% to 7% for a substrate with wrinkles or ripples and from 4% to 22% for a substrate with wrinkles or ripples which also contained a fold in its structure. The increase in light absorption occurred because light that reaches to the detector was trapped between rip-

Table 2
Graphene oxide based biosensors for detection of different targets. GO: Graphene oxide, GOD: Glucose oxidase enzyme, PAMAM: Poly (amidoamine), Au NPs: Gold nanoparticles, Ag NPs: Silver nanoparticles, ss-DNA: single stranded DNA, ds-DNA : Double stranded DNA, IgG: Immunoglobulin G.

Sensor Type	Target	Detection Method	Reference
Electrochemical	Glucose	GO/ GOD	[112]
Electrochemical	Vascular endothelial growth factor	Magnetic GO/Au electrode surface/Avastin	[113]
Electrochemical	Estradiol	Graphene/Polyaniline/ PAMAM/Au Ps/Peroxidase/GO/Antibody	[114]
Electrochemical	DNA	ATP-GO/Au NPs/ss-DNA probe/Glassy carbon electrode	[115]
Electrochemical	Pb(II), Cu(II) and Hg(II)	GO/L-cysteine modidifed Au NPs/Au electrode	[116]
Fluorescent	DNA	GO/Reduced graphene quantum dots/ssDNA	[117]
Fluorescent	Helicase activity	GO/dsDNA	[118]
Fluorescent	Dopamine	Fluorescently labeled GO	[119]
Fluorescent	Thrombin	DNA aptamer/GO/N-methyl-mesoporpyrin	[120]
Fluorescent	Pb(II)	GO/dye labeled anticancer drug AGRO100 aptamer	[121]
Surface Plasmon Resonance	Lysozyme	GO-coated SPR/Micrococcus lysodeikticus/Poly(diallyldimethylamonium)	[122]
Surface Plasmon Resonance	MicroRNA	GO/Au NPs/ssDNA	[123]
Surface Plasmon Resonance	IgG	GO silica fiber/silver	[124]
Surface Plasmon Resonance	Cytokeratin	GO/Au layer/antibody	[125]
Surface-Enhanced Raman Scattering	DNA	GO/ssDNA/Ag NPs/Cy3	[126]
Surface-Enhanced Raman Scattering	Cardiac troponin I	GO/Au-antibody/Malachite green isothiocyanate	[127]
Surface-Enhanced Raman Scattering	prostate specific antigen	GO/Ag NPs/Antibody	[128]
Surface-Enhanced Raman Scattering	IgG	GO/Antibody/Au NPs/magnetic bead	[129]
Optical	Hemoglobin	GO/Long period grating	[130]
Optical	Ammonia gas	GO/ZnO/Microfiber interferometer	[131]

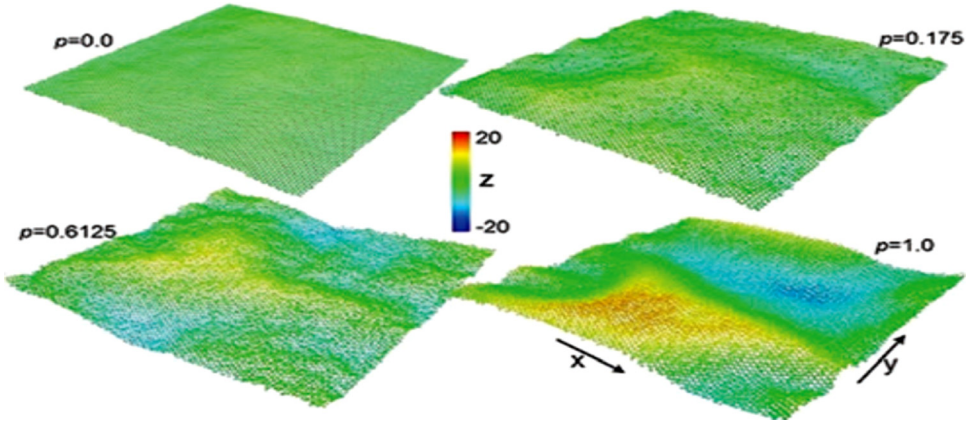

Fig. 18. Oxidation degree-rippling effect relationship. As p represents the oxidation degree and z represents the out-of-plane elevation, when p = 0.0 there is almost no ripple on the graphene oxide z is close to zero. However, as oxidation degree increases and become p = 1.0 there are lots of ripples on the surface and z value becomes almost 20 or −20 [132].

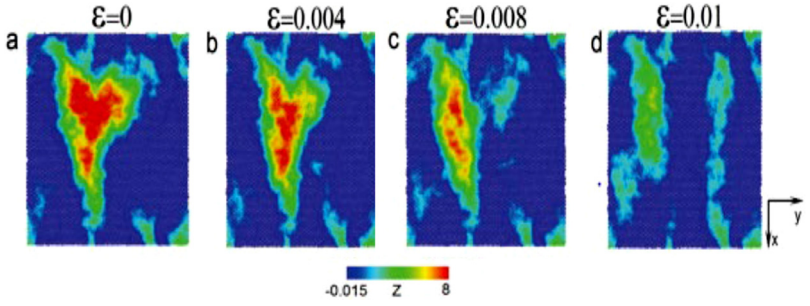

Fig. 19. Positive and Negative Poisson's Ratio. If the ratio is positive, when material is stretched in x direction, in response to this, material is compressed in y direction. If the ratio is negative, when material is stretched in x direction, in response to this, material is also stretched in y direction [147].

ples [138]. It is assumed that a similar effect can be observed in graphene oxide based devices.

6.1.3. Conductivity

As mentioned previously, conductivity of GO is low but can be improved by combining it with conductive materials. In order to increase the area to immobilize more bioreceptor molecules, rippled and wrinkled GO surface can be used [139].

For example, Ali et al. (2016) produced a nitrate detection biosensor based on GO and gold nanoparticles (Au NPs). They put GO onto substrate polydimethylsiloxane (PDMS) and covered it with Au NPs to improve conductivity. Then, they pre-stretched this composite and produce a rippled and wrinkled surface. The rippled/wrinkled surface area increased the electroactive surface area and more enzyme (nitrate reductase) could be immobilized on the nanocomposite surface. It also had a higher electron transfer rate and enhanced the diffusibility of the electrons produced from catalytic reactions. In the experiment, when a pre-stretched value of 8.0% was applied, peak current (sensitivity) increased as immobilized enzyme volume increased. When enzyme saturation

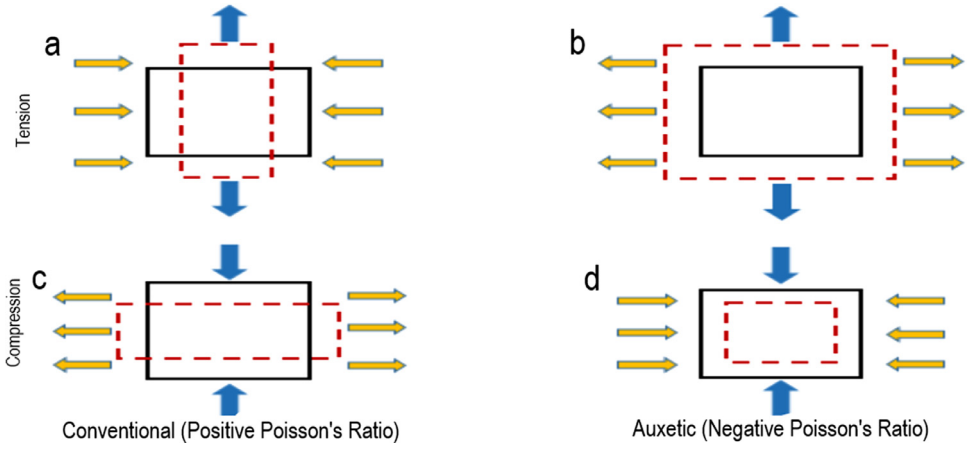

Fig. 20. Effects of different values of strain to the ripples under the same oxidation degree. When oxidation degree is high (p = 0.6125) GO has NPR. As GO is stretched in x direction, y direction of GO is also stretched and the amplitudes of the ripples decrease as it is indicated in topography map [132].

Table 3
Ripples effect on different graphene biosensing concepts.

Biosensor Type	Affected Property	Ripple effect	Reference
Electrochemical	Electroctalytic activity Immobilization rate Hybridization efficiency Catalytic activity	Ripples on graphene structure cause Au nanoparticles to form Au nanorods on the surface which increase the composite's electrocatalytic capability at the end. Combination of formed Au nanorods and large surface area causes improvement of self-assembled monolayer that as a result causes increase in immobilization rates and hybridization efficiency. Au nanorods/graphene composite also provides high surface areas and specificity (SSA), high mechanical strength, enhanced catalytic activity and fast electron transfer.	[78]
Surface-enhanced Raman Spectroscopy	Light absorption Light matter interaction Local electromagnetic field	Experiment demonstrates that ripples enhance the SERS properties compared to planar graphene. When monolayer graphene assembled on an Au/Ag core-shell, it improves the light-matter interaction in the sensor and adjusts light absorption of graphene as a result of the formed ripples. Ripples also provide improvement of local electromagnetic field that enhances the excitation of the molecule. It is observed that ripples with shorter wavelengths (λ < 600 nm) enhance field intensity more than ripples with longer wavelengths (λ > 800 nm).	[141]
Surface plasmon resonance	Plasmonic coupling High-spot density	For better local surface plasmon resonance applications, plasmonic coupling is required. In graphene biosensing applications ripples can be used in order to increase the enhancement factor (EF) of the plasmonic coupling. When multilayer graphene/Au NPs possesses ripples, the spatial separation between nanoparticles may be diminished and this causes the improved near-field enhancement in addition to the increase in high-spot density in z-direction.	[142]
Fluorescent	Quenching	Ripples improve the fluorophore quenching ability of graphene oxide. So the rippled areas of graphene oxide can quench the fluorophores more effectively than planar parts.	[111]

occurred, the maximum peak was observed. Thus, by modifying the number and amplitude of the wrinkles/ripples on the graphene surface, electrochemical current and sensitivity of the electrode can be adjusted [140].

6.1.4. Fluorescence quenching

Fluorescence quenching is one of the most important properties of graphene oxide, resulting in its use in fluorescence based biosensors. Li et al. (2018) observed that when graphene oxide contains ripples/wrinkles in its structure, effectivity of fluorophore quenching of GO increased. Thus, rippled GO has a higher quenching ability than flat GO [111].

In summary, to understand the ripples effect on different graphene biosensing concepts following Table 3 can be examined:

Future Opportunities

Graphene and its derivatives have become significant materials in biosensing applications in the last few decades. Graphene's outstanding electrical, mechanical and chemical properties improve the efficiency of biosensors. Since graphene possesses so many unique properties to be exploited in biosensors, further investigations are warranted. Out-of-plane structures called 'ripples' on graphene have only recently been discovered, therefore, there are still unknown effects of these structures on graphene properties. Although ripples improve flexibility and surface area of graphene, they also have some adverse effects like decreasing mechanical strength and electrical conductivity [80,23]. Since ripples are primarily intrinsic with both negative and positive effects, it will be necessary to tailor ripples on graphene in order to achieve the specific optimum properties required in a given biosensing application. We believe that discovering the nature of graphene ripples can improve the bio-detection quality and efficiency in a variety of areas including medicine and the food industry.

In some cases, ripples improve specific properties of the graphene so that the increase in the number of ripples is beneficial. For instance, in wearable biosensors being flexible is more important than a decrease in electrical conductivity which can be

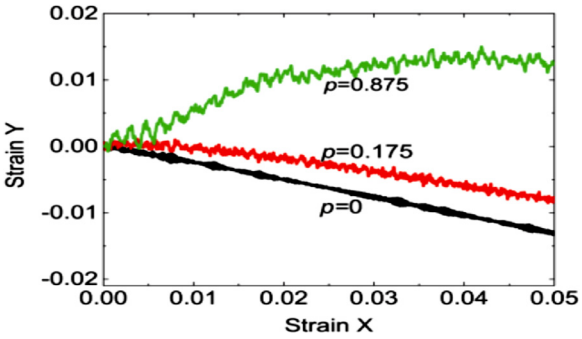

Fig. 21. Relationship between oxidation degree and the Poisson's ratio. As degree of oxidation in GO increases the Poisson's ratio decreases and become negative. In opposite, as degree of oxidation in GO decreases the Poisson's ratio become positive [132].

overlooked to some degree. In contrast, if having high conductivity is more significant than being flexible, ripples should be avoided as much as possible. As a result, further research must be conducted on the effect that ripples have on graphene properties, which would facilitate the production of optimum biosensing devices using graphene.

Ripples can be modified using a variety of different methods such as the thermal, chemical or mechanical techniques discussed above [8]. Using such techniques to achieve a specific number or size of ripples, or to fully remove them, is a difficult prospect and further research is necessary in this field. In particular, the development of more simplistic techniques for the manipulation of ripples would be of benefit. By optimizing processes that modify ripples, the specific properties required for a biosensing application could be attained and the graphene structure more easily handled. In conclusion, although more research is required on ripple modification, graphene and its derivatives show great promise and their use in biosensing applications will only increase in the future.

Declaration of Competing Interest

The authors declare that they have no known competing financial interests or personal relationships that could have appeared to influence the work reported in this paper.

References

[1] M. Pohanka, Current trends in the biosensors for biological warfare agents assay, Materials (Basel) 12 (2019), doi:10.3390/ma12142303.
[2] N. Bhalla, P. Jolly, N. Formisano, P. Estrela, Introduction to biosensors, (2016) 1–8. doi:10.1042/EBC20150001.
[3] O. Lazcka, F.J. Del Campo, F.X. Muñoz, Pathogen detection: a perspective of traditional methods and biosensors, Biosens. Bioelectron. 22 (2007) 1205–1217, doi:10.1016/j.bios.2006.06.036.
[4] S.M.Z. Hossain, N. Mansour, Biosensors for on-line water quality monitoring–a review, Arab J. Basic Appl. Sci. 26 (2019) 502–518, doi:10.1080/25765299.2019.1691434.
[5] S. Lanzalaco, G.M. Brenda, Polymers and Plastics Modified Electrodes for Biosensors: a Review, Molecules 25 (10) (2020) 2446.
[6] S. Zhang, G. Wright, Y. Yang, Materials and techniques for electrochemical biosensor design and construction, Biosens. Bioelectron. 15 (5–6) (2000) 273–282.
[7] A. Fasolino, J.H. Los, M.I. Katsnelson, Intrinsic ripples in graphene, Nat. Mater. 6 (2007) 858–861, doi:10.1038/nmat2011.
[8] W. Bao, F. Miao, Z. Chen, H. Zhang, W. Jang, C. Dames, C.N. Lau, Controlled ripple texturing of suspended graphene and ultrathin graphite membranes, Nat. Nanotechnol. 4 (2009) 562–566, doi:10.1038/nnano.2009.191.
[9] R.K. Gautam, A. Verma, Electrocatalyst Materials for Oxygen Reduction Reaction in Microbial Fuel Cell, Elsevier B.V., 2019, doi:10.1016/b978-0-444-64052-9.00018-2.
[10] S. Banerjee, J.H. Lee, T. Kuila, N.H. Kim, 7 - Synthesis of Graphene-Based Polymeric Nanocomposites, Elsevier Ltd, 2007, doi:10.1016/B978-0-08-100079-3.00007-7.
[11] J.F. Dai, G.J. Wang, L. Ma, C.K. Wu, Surface properties of graphene: relationship to graphene-polymer composites, Rev. Adv. Mater. Sci. 40 (2015) 60–71.
[12] B. Alemour, M.H. Yacoob, H.N. Lim, M.R. Hassan, Review of Electrical Properties of Graphene Conductive Composites, International Journal of Nanoelectronics & Materials 11 (4) (2018).
[13] J. Wang, F. Ma, W. Liang, M. Sun, Electrical properties and applications of graphene, hexagonal boron nitride (h-BN), and graphene/h-BN heterostructures, Mater. Today Phys. 2 (2017) 6–34, doi:10.1016/j.mtphys.2017.07.001.
[14] T. Onishi, Chapter 2 - Quantum, Chemistry in Functional Inorganic Materials, 1st ed., Elsevier Inc., 2012, doi:10.1016/B978-0-12-396498-4.00002-8.
[15] Z. Jiang, Y. Zhang, Y.W. Tan, H.L. Stormer, P. Kim, Quantum Hall effect in graphene, Solid State Commun 143 (2007) 14–19, doi:10.1016/j.ssc.2007.02.046.
[16] D.H. Chae, T. Utikal, S. Weisenburger, H. Giessen, K.V. Klitzing, M. Lippitz, J. Smet, Excitonic fano resonance in free-standing graphene, Nano Lett. 11 (3) (2011) 1379–1382, doi:10.1021/nl200040q.
[17] E.N. Koukaras, G. Kalosakas, C. Galiotis, Phonon properties of graphene derived from molecular dynamics simulations, Nat. Publ. Gr. (2015), doi:10.1038/srep12923.
[18] M.J. Baker, J. Trevisan, P. Bassan, R. Bhargava, H.J. Butler, K.M. Dorling, P.R. Fielden, S.W. Fogarty, N.J. Fullwood, K.A. Heys, C. Hughes, P. Lasch, P.L. Martin-hirsch, B. Obinaju, G.D. Sockalingum, J. Sulé-suso, R.J. Strong, M.J. Walsh, B.R. Wood, P. Gardner, F.L. Martin, Using Fourier transform IR spectroscopy to analyze biological materials, 9 (2014) 1771–1791. doi:10.1038/nprot.2014.110.
[19] M.F. Craciun, S. Russo, M. Yamamoto, S. Tarucha, Tuneable electronic properties in graphene, Nano Today 6 (2011) 42–60, doi:10.1016/j.nantod.2010.12.001.
[20] Y. Zhu, S. Murali, W. Cai, X. Li, J.W. Suk, J.R. Potts, R.S. Ruoff, Graphene and graphene oxide: synthesis, properties, and applications, Adv. Mater. 22 (2010) 3906–3924, doi:10.1002/adma.201001068.
[21] J. Peña-Bahamonde, H.N. Nguyen, S.K. Fanourakis, D.F. Rodrigues, Recent advances in graphene-based biosensor technology with applications in life sciences, J. Nanobiotechnology. 16 (2018) 1–17, doi:10.1186/s12951-018-0400-z.
[22] N. Chauhan, T. Maekawa, D.N.S. Kumar, Graphene based biosensors - Accelerating medical diagnostics to new-dimensions, J. Mater. Res. 32 (2017) 2860–2882, doi:10.1557/jmr.2017.91.
[23] Y. Bai, T. Xu, X. Zhang, Graphene-based biosensors for detection of biomarkers, Micromachines (Basel) 11 (1) (2020) 60, doi:10.3390/mi11010060.
[24] V. Georgakilas, M. Otyepka, A.B. Bourlinos, V. Chandra, N. Kim, K.C. Kemp, P. Hobza, R. Zboril, K.S. Kim, Functionalization of Graphene : covalent and Non-Covalent Approaches , Derivatives and Applications, Chem. Rev. 112 (11) (2012) 6156–6214, doi:10.1021/cr3000412.
[25] D. Li, W. Zhang, X. Yu, Z. Wang, Z. Su, G. Wei, When biomolecules meet graphene: from molecular level interactions to material design and applications, Nanoscale 8 (47) (2016) 19491–19509, doi:10.1039/C6NR07249F.
[26] M. Pumera, Graphene in biosensing, Mater. Today 14 (2011) 308–315, doi:10.1016/S1369-7021(11)70160-2.
[27] J. Ortiz Balbuena, P. Tutor De Ureta, E.R. Ruiz, S. Mellor Pita, Enfermedad de Vogt-Koyanagi-Harada, Med. Clin. (Barc). 146 (2016) 93–94, doi:10.1016/j.medcli.2015.04.005.
[28] A.C.B. Dias, R.A.O. Silva, M.A.Z. Arruda, A sequential injection system for indirect spectrophotometric determination of lactic acid in yogurt and fermented mash samples, Microchem. J. 96 (2010) 151–156, doi:10.1016/j.microc.2010.02.016.
[29] F. Yamasaki, K. Kurisu, Y. Kajiwara, Y. Watanabe, T. Takayasu, Y. Akiyama, T. Saito, R. Hanaya, K. Sugiyama, Magnetic resonance spectroscopic detection of lactate is predictive of a poor prognosis in patients with diffuse intrinsic pontine glioma, Neuro. Oncol. 13 (2011) 791–801, doi:10.1093/neuonc/nor038.
[30] H. Henry, N. Marmy Conus, P. Steenhout, A. Béguin, O. Boulat, Sensitive determination of D-lactic acid and L-lactic acid in urine by high-performance liquid chromatography-tandem mass spectrometry, Biomed. Chromatogr. 26 (2012) 425–428, doi:10.1002/bmc.1681.
[31] V. Casimiri, C. Burstein, Biosensor for L-lactate determination as an index of E. coli number in crude culture medium, Anal. Chim. Acta. 361 (1998) 45–53, doi:10.1016/S0003-2670(98)00011-7.
[32] P. Labroo, Y. Cui, Flexible graphene bio-nanosensor for lactate, Biosens. Bioelectron. 41 (2013) 852–856, doi:10.1016/j.bios.2012.08.024.
[33] W. Zhang, Y. Du, M.L. Wang, Noninvasive glucose monitoring using saliva nano-biosensor, Sens. Bio-Sensing Res. 4 (2015) 23–29, doi:10.1016/j.sbsr.2015.02.002.
[34] X. Kang, J. Wang, H. Wu, I.A. Aksay, J. Liu, Y. Lin, Glucose Oxidase-graphene-chitosan modified electrode for direct electrochemistry and glucose sensing, Biosens. Bioelectron. 25 (2009) 901–905, doi:10.1016/j.bios.2009.09.004.
[35] K. Mao, D. Wu, Y. Li, H. Ma, Z. Ni, H. Yu, C. Luo, Q. Wei, B. Du, Label-free electrochemical immunosensor based on graphene/methylene blue nanocomposite, Anal. Biochem. 422 (2012) 22–27, doi:10.1016/j.ab.2011.12.047.
[36] W. Yang, K.R. Ratinac, S.R. Ringer, P. Thordarson, J.J. Gooding, F. Braet, Carbon nanomaterials in biosensors: should you use nanotubes or graphene, Angew. Chemie - Int. Ed. 49 (2010) 2114–2138, doi:10.1002/anie.200903463.
[37] C. Wang, X. Cui, Y. Li, H. Li, L. Huang, J. Bi, J. Luo, L.Q. Ma, W. Zhou, Y. Cao, B. Wang, F. Miao, A label-free and portable graphene FET aptasensor for children blood lead detection, Sci. Rep. 6 (2016) 1–8, doi:10.1038/srep21711.
[38] S.P. Ng, G. Qiu, N. Ding, X. Lu, C.M.L. Wu, Label-free detection of 3-nitro-L-tyrosine with nickel-doped graphene localized surface plasmon resonance biosensor, Biosens. Bioelectron. 89 (2017) 468–476, doi:10.1016/j.bios.2016.04.017.
[39] L. He, Q. Pagneux, I. Larroulet, A.Y. Serrano, A. Pesquera, A. Zurutuza, D. Mandler, R. Boukherroub, S. Szunerits, Label-free femtomolar cancer biomarker

detection in human serum using graphene-coated surface plasmon resonance chips, Biosens. Bioelectron. 89 (2017) 606–611, doi:10.1016/j.bios.2016.01.076.
[40] B.A. Prabowo, A. Alom, M.K. Secario, F.C.P. Masim, H.C. Lai, K. Hatanaka, K.C. Liu, Graphene-based Portable SPR Sensor for the Detection of Mycobacterium tuberculosis DNA Strain, Procedia Eng 168 (2016) 541–545, doi:10.1016/j.proeng.2016.11.520.
[41] L. Ouyang, Q. Zhang, G. Ma, L. Zhu, Y. Wang, Z. Chen, Y. Wang, L. Zhao, New Dual-Spectroscopic Strategy for the Direct Detection of Aristolochic Acids in Blood and Tissue, Anal. Chem. 91 (2019) 8154–8161, doi:10.1021/acs.analchem.9b00442.
[42] S. Feng, M. Cristina dos Santos, B.R. Carvalho, R. Lv, Q. Li, K. Fujisawa, A.L. Elías, Y. Lei, N. Perea-López, M. Endo, M. Pan, M.A. Pimenta, M. Terrones, Ultrasensitive molecular sensor using N-doped graphene through enhanced Raman scattering, Sci. Adv. 2 (2016) 1–13, doi:10.1126/sciadv.1600322.
[43] C. Zhang, B. Man, Z. Li, X. Xiu, L. Hou, J. Yu, S. Jiang, X. Zhao, Q. Peng, S. Qiu, C. Li, Manipulating the surface-enhanced Raman spectroscopy (SERS) activity and plasmon-driven catalytic efficiency by the control of Ag NP/graphene layers under optical excitation, Nanophotonics 10 (2021) 1529–1540, doi:10.1515/nanoph-2020-0644.
[44] N. Li, T. Tang, J. Li, L. Luo, C. Li, J. Shen, J. Yao, Highly sensitive biosensor with graphene-MoS2 heterostructure based on photonic spin Hall effect, J. Magn. Magn. Mater. 484 (2019) 445–450, doi:10.1016/j.jmmm.2019.04.003.
[45] P.N.S.S. Ja'Afar, N.M. Razali, N.F.A. Zaidi, F. Ahmad, M.F. Omar, A.K. Ismail, N. Rosdi, M.H. Yaacob, A. Hamzah, H.M. Kaidi, S. Ambran, Graphene coated optical fiber tip sensor for nitrate sensing application, in: 2020 IEEE 8th Int. Conf. Photonics, ICP 2020, 2020, pp. 3–4, doi:10.1109/ICP46580.2020.9206450.
[46] S. Deng, V. Berry, Wrinkled, rippled and crumpled graphene: an overview of formation mechanism, electronic properties, and applications, Mater. Today. 19 (2016) 197–212, doi:10.1016/j.mattod.2015.10.002.
[47] C.H. Lui, L. Liu, K.F. Mak, G.W. Flynn, T.F. Heinz, Ultraflat graphene, Nature 462 (2009) 339–341, doi:10.1038/nature08569.
[48] J. Wang, H.A. Fertig, G. Murthy, L. Brey, Excitonic effects in two-dimensional massless Dirac fermions, Phys. Rev. B 83 (3) (2011) 035404, doi:10.1103/PhysRevB.83.035404.
[49] R. Bala, A. Marwaha, S. Marwaha, Comparative analysis of zigzag and armchair structures for graphene patch antenna in THz band, J. Mater. Sci. Mater. Electron. (2016), doi:10.1007/s10854-016-4394-8.
[50] J.S. Choi, Y.J. Chang, S. Woo, Y. Son, Y. Park, M.J. Lee, I. Byun, J. Kim, C. Choi, A. Bostwick, E. Rotenberg, B.H. Park, Correlation between micrometer-scale ripple alignment and atomic-scale crystallographic orientation of monolayer graphene, (2014) 1–5. doi:10.1038/srep07263.
[51] Y. Park, J.S. Choi, T. Choi, M.J. Lee, Q. Jia, M. Park, Configuration of ripple domains and their topological defects formed under local mechanical stress on hexagonal monolayer graphene, (2015). https://doi.org/10.1038/srep09390.
[52] M.A. Hopcroft, W.D. Nix, T.W. Kenny, What is the Young's Modulus of Silicon? J. Microelectromech. Syst. 19 (2) (2010) 229–238.
[53] D.G. Papageorgiou, I.A. Kinloch, R.J. Young, Progress in Materials Science Mechanical properties of graphene and graphene-based nanocomposites, Prog. Mater. Sci. 90 (2017) 75–127, doi:10.1016/j.pmatsci.2017.07.004.
[54] Z. Pavlík, M. Pavlíková, M. Záleská, Properties of concrete with plastic polypropylene aggregates, Use Recycl. Plast. Eco-Efficient Concr. (2019) 189–213, doi:10.1016/b978-0-08-102676-2.00009-8.
[55] Q. Cao, X. Geng, H. Wang, P. Wang, A. Liu, Y. Lan, Q. Peng, A review of current development of graphene mechanics, Crystals 8 (9) (2018) 357, doi:10.3390/cryst8090357.
[56] S. Lee, Effect of Intrinsic Ripples on Elasticity of the Graphene Monolayer, Nanoscale Res. Lett. 10 (2015), doi:10.1186/s11671-015-1135-5.
[57] C.M. González-Henríquez, M.A. Sarabia Vallejos, J. Rodríguez-Hernández, Introduction to surface instabilities and wrinkle formation, Wrinkled Polym. Surfaces Strateg. Methods Appl. 3 (2019), doi:10.1007/978-3-030-05123-5.
[58] R. Miranda, A.L. Vázquez De Parga, Graphene: surfing ripples towards new devices, Nat. Nanotechnol. 4 (2009) 549–550, doi:10.1038/nnano.2009.250.
[59] G. Gui, J. Zhong, Z. Ma, Electronic properties of rippled graphene, J. Phys. Conf. Ser. 402 (2012), doi:10.1088/1742-6596/402/1/012004.
[60] E.A. Kim, A.H. Castro Neto, Graphene as an electronic membrane, Epl 84 (2008) 2–7, doi:10.1209/0295-5075/84/57007.
[61] A.H. Castro Neto, F. Guinea, N.M.R. Peres, K.S. Novoselov, A.K. Geim, The electronic properties of graphene, Rev. Mod. Phys. 81 (2009) 109–162, doi:10.1103/RevModPhys.81.109.
[62] D.B. Zhang, E. Akatyeva, T. Dumitric, Bending ultrathin graphene at the margins of continuum mechanics, Phys. Rev. Lett. 106 (2011) 3–6, doi:10.1103/PhysRevLett.106.255503.
[63] M. Zwierzycki, Transport properties of rippled graphene, J. Phys. Condens. Matter. 26 (2014), doi:10.1088/0953-8984/26/13/135303.
[64] I. Yudhistira, S. Adam, Theory for electron transport in graphene, Synth. Met. 210 (2015) 2–8, doi:10.1016/j.synthmet.2015.07.027.
[65] M. Peplow, Graphene: the quest for supercarbon, Nature 503 (2013) 327–329, doi:10.1038/503327a.
[66] G. Gui, D. Morgan, J. Booske, J. Zhong, Z. Ma, Local strain effect on the band gap engineering of graphene by a first-principles study, Appl. Phys. Lett. 106 (2015), doi:10.1063/1.4907410.
[67] G. Gui, J. Zhong, Z. Ma, Electronic properties of rippled graphene, J. Phys. Conf. Ser. 402 (2012) 1–5, doi:10.1088/1742-6596/402/1/012004.
[68] J. Aljedani, M.J. Chen, B.J. Cox, Variational model for a rippled graphene sheet, RSC Adv 10 (2020) 16016–16026, doi:10.1039/c9ra10439a.
[69] I.Y. Sahalianov, T.M. Radchenko, V.A. Tatarenko, G. Cuniberti, Y.I. Prylutskyy, Straintronics in graphene: extra large electronic band gap induced by tensile and shear strains, J. Appl. Phys. 126 (2019), doi:10.1063/1.5095600.
[70] C.W. Chiang, G. Haider, W.C. Tan, Y.R. Liou, Y.C. Lai, R. Ravindranath, H.T. Chang, Y.F. Chen, Highly Stretchable and Sensitive Photodetectors Based on Hybrid Graphene and Graphene Quantum Dots, ACS Appl. Mater. Interfaces. 8 (2016) 466–471, doi:10.1021/acsami.5b09373.
[71] Y. Wang, R. Yang, Z. Shi, L. Zhang, D. Shi, E. Wang, G. Zhang, Super-elastic graphene ripples for flexible strain sensors, ACS Nano 5 (2011) 3645–3650, doi:10.1021/nn103523t.
[72] Y. Chan, M. Skreta, H. McPhee, S. Saha, R. Deus, L. Soleymani, Solution-processed wrinkled electrodes enable the development of stretchable electrochemical biosensors, Analyst 144 (2019) 172–179, doi:10.1039/c8an01637b.
[73] Y.C. Lai, Y.C. Huang, T.Y. Lin, Y.X. Wang, C.Y. Chang, Y. Li, T.Y. Lin, B.W. Ye, Y.P. Hsieh, W.F. Su, Y.J. Yang, Y.F. Chen, Stretchable organic memory: toward learnable and digitized stretchable electronic applications, NPG Asia Mater 6 (2014) 1–7, doi:10.1038/am.2013.85.
[74] K.S. Kim, Y. Zhao, H. Jang, S.Y. Lee, J.M. Kim, K.S. Kim, J.H. Ahn, P. Kim, J.Y. Choi, B.H. Hong, Large-scale pattern growth of graphene films for stretchable transparent electrodes, Nature 457 (2009) 706–710, doi:10.1038/nature07719.
[75] H. Wu, J. Wang, X. Kang, C. Wang, D. Wang, J. Liu, I.A. Aksay, Y. Lin, Glucose biosensor based on immobilization of glucose oxidase in platinum nanoparticles/graphene/chitosan nanocomposite film, Talanta 80 (2009) 403–406, doi:10.1016/j.talanta.2009.06.054.
[76] M. Carbone, L. Gorton, R. Antiochia, An overview of the latest graphene-based sensors for glucose detection: the effects of graphene defects, Electroanalysis 27 (2015) 16–31, doi:10.1002/elan.201400409.
[77] J. Hui, J. Cui, G. Xu, S.B. Adeloju, Y. Wu, Direct electrochemistry of glucose oxidase based on Nafion-Graphene-GOD modified gold electrode and application to glucose detection, Mater. Lett. 108 (2013) 88–91, doi:10.1016/j.matlet.2013.06.097.
[78] V. Perumal, M.S.M. Saheed, N.M. Mohamed, M.S.M. Saheed, S.S. Murthe, S.C.B. Gopinath, J.M. Chiu, Gold nanorod embedded novel 3D graphene nanocomposite for selective bio-capture in rapid detection of Mycobacterium tuberculosis, Biosens. Bioelectron. 116 (2018) 116–122, doi:10.1016/j.bios.2018.05.042.
[79] R.C. Adams-McGavin, Y. Chan, C.M. Gabardo, J. Yang, M. Skreta, B.C. Fung, L. Soleymani, Nanoporous and wrinkled electrodes enhance the sensitivity of glucose biosensors, Electrochim. Acta. 242 (2017) 1–9, doi:10.1016/j.electacta.2017.04.108.
[80] C.N.R. Rao, A.K. Sood, K.S. Subrahmanyam, A. Govindaraj, Graphene : the New Two-Dimensional Nanomaterial, Angew. Chem. Int. Ed. (2009) 7752–7777, doi:10.1002/anie.200901678.
[81] H. Lee, I. Kim, M. Kim, H. Lee, Moving beyond flexible to stretchable conductive electrodes using metal nanowires and graphenes, Nanoscale 8 (2016) 1789–1822, doi:10.1039/c5nr06851g.
[82] Q. Su, S.J. Koester, Understanding Sources of Electrical Disorder in Graphene Grown by Chemical Vapor Deposition for Wafer-Scale Device Applications, ACS Appl. Nano Mater. 2 (2019) 3426–3433, doi:10.1021/acsanm.9b00350.
[83] E.P. Nguyen, C. De Carvalho Castro Silva, A. Merkoçi, Recent advancement in biomedical applications on the surface of two-dimensional materials: from biosensing to tissue engineering, Nanoscale 12 (2020) 19043–19067, doi:10.1039/d0nr05287f.
[84] B. Li, Y. Zhang, X.Y. Meng, R. Zhou, Zipper-Like Unfolding of dsDNA Caused by Graphene Wrinkles, J. Phys. Chem. C. 124 (2020) 3332–3340, doi:10.1021/acs.jpcc.9b08778.
[85] R. Banerjee, V.H. Nguyen, T. Granzier-Nakajima, L. Pabbi, A. Lherbier, A.R. Binion, J.C. Charlier, M. Terrones, E.W. Hudson, Strain Modulated Superlattices in Graphene, Nano Lett 20 (2020) 3113–3121, doi:10.1021/acs.nanolett.9b05108.
[86] M. Kowalik, M.J. Hossain, A. Lele, W. Zhu, R. Banerjee, T. Granzier-Nakajima, M. Terrones, E.W. Hudson, A.C.T. van Duin, Atomistic-scale simulations on graphene bending near a copper surface, Catalysts 11 (2021) 1–12, doi:10.3390/catal11020208.
[87] D.D.L. Chung, Polymer-Matrix Composites: Mechanical Properties and Thermal Performance, Second Edi, Elsevier Inc., 2017, doi:10.1016/b978-0-12-804459-9.00004-x.
[88] W. Gao, R. Huang, Thermomechanics of monolayer graphene: rippling, thermal expansion and elasticity, J. Mech. Phys. Solids. 66 (2014) 42–58, doi:10.1016/j.jmps.2014.01.011.
[89] M. Zahabul Islam, M. Mahboob, L. Robert Lowe, E. Stephen Bechtel, Characterization of the thermal expansion properties of graphene using molecular dynamics simulations, J. Phys. D. Appl. Phys. 46 (2013) 2–7, doi:10.1088/0022-3727/46/43/435302.
[90] M. Annamalai, S. Mathew, M. Jamali, D. Zhan, M. Palaniapan, Effects of annealing on the ripple texture and mechanical properties of suspended bilayer graphene, J. Phys. D. Appl. Phys. 46 (2013), doi:10.1088/0022-3727/46/14/145302.
[91] Z. Juang, C. Wu, A. Lu, C. Su, K. Leou, Graphene synthesis by chemical vapor deposition and transfer by a roll-to-roll process Zhen-Yu Juang *, Chih-Yu Wu, Ang-Yu Lu, Ching-Yuan Su, Keh-Chyang Leou, Fu-Rong Chen, Chuen-Horng Tsai, Carbon N. Y. (2010) 1–19 [cond-mat.mtrl-sci] arXiv:1005.1510v1 . [cond-mat.mtrl-sci] http://aps.arxiv.org/ftp/arxiv/papers/1005/1005.1510.pdf .
[92] W. Xueshen, L. Jinjin, Z. Qing, Z. Yuan, Z. Mengke, Thermal annealing of exfoliated graphene, J. Nanomater. 2013 (2013), doi:10.1155/2013/101765.

[93] M.M.M. Alyobi, C.J. Barnett, R.J. Cobley, Effects of thermal annealing on the properties of mechanically exfoliated suspended and on-substrate few-layer graphene, Crystals 7 (2017) 1–11, doi:10.3390/cryst7110349.
[94] F. Perrozzi, S. Prezioso, L. Ottaviano, Graphene oxide: from fundamentals to applications, J. Phys. Condens. Matter. 27 (2015) 13002, doi:10.1088/0953-8984/27/1/013002.
[95] O.C. Compton, S.T. Nguyen, Graphene oxide, highly reduced graphene oxide, and graphene: versatile building blocks for carbon-based materials, Small 6 (2010) 711–723, doi:10.1002/smll.200901934.
[96] Z.U. Khan, A. Kausar, H. Ullah, A. Badshah, W.U. Khan, A review of graphene oxide, graphene buckypaper, and polymer/graphene composites: properties and fabrication techniques, J. Plast. Film Sheeting. 32 (2016) 336–379, doi:10.1177/8756087915614612.
[97] A.R. Khoei, M.S. Khorrami, Mechanical properties of graphene oxide: a molecular dynamics study, Fullerenes Nanotub. Carbon Nanostructures. 24 (2016) 594–603, doi:10.1080/1536383X.2016.1208180.
[98] A. Vaidya, K. Pathak, Mechanical Stability of Dental Materials, Elsevier Inc., 2018, doi:10.1016/B978-0-12-813742-0.00017-1.
[99] A.T. Smith, A.M. LaChance, S. Zeng, B. Liu, L. Sun, Synthesis, properties, and applications of graphene oxide/reduced graphene oxide and their nanocomposites, Nano Mater. Sci. 1 (2019) 31–47, doi:10.1016/j.nanoms.2019.02.004.
[100] X. Mu, X. Wu, T. Zhang, D.B. Go, T. Luo, Thermal transport in graphene oxide - From ballistic extreme to amorphous limit, Sci. Rep. 4 (2014) 1–9, doi:10.1038/srep03909.
[101] D. Chen, H. Feng, J. Li, Graphene oxide: preparation, functionalization, and electrochemical applications, Chem. Rev. 112 (2012) 6027–6053, doi:10.1021/cr300115g.
[102] K. Erickson, R. Erni, Z. Lee, N. Alem, W. Gannett, A. Zettl, Determination of the local chemical structure of graphene oxide and reduced graphene oxide, Adv. Mater. 22 (2010) 4467–4472, doi:10.1002/adma.201000732.
[103] S.K. Krishnan, E. Singh, P. Singh, M. Meyyappan, H.S. Nalwa, A review on graphene-based nanocomposites for electrochemical and fluorescent biosensors, RSC Adv 9 (2019) 8778–8781, doi:10.1039/c8ra09577a.
[104] B.M. Ganesh, A.M. Isloor, A.F. Ismail, Enhanced hydrophilicity and salt rejection study of graphene oxide-polysulfone mixed matrix membrane, Desalination 313 (2013) 199–207, doi:10.1016/j.desal.2012.11.037.
[105] J. Lee, H.R. Chae, Y.J. Won, K. Lee, C.H. Lee, H.H. Lee, I.C. Kim, J. min Lee, Graphene oxide nanoplatelets composite membrane with hydrophilic and antifouling properties for wastewater treatment, J. Memb. Sci. 448 (2013) 223–230, doi:10.1016/j.memsci.2013.08.017.
[106] P.T. Yin, S. Shah, M. Chhowalla, K.B. Lee, Design, synthesis, and characterization of graphene-nanoparticle hybrid materials for bioapplications, Chem. Rev. 115 (2015) 2483–2531, doi:10.1021/cr500537t.
[107] J. Lee, J. Kim, S. Kim, D.H. Min, Biosensors based on graphene oxide and its biomedical application, Adv. Drug Deliv. Rev. 105 (2016) 275–287, doi:10.1016/j.addr.2016.06.001.
[108] R.S. Swathi, K.L. Sebastian, Resonance energy transfer from a dye molecule to graphene, J. Chem. Phys. 129 (2008), doi:10.1063/1.2956498.
[109] M. De Miguel, M. Aílvaro, H. Garciía, Graphene as a quencher of electronic excited states of photochemical probes, Langmuir 28 (2012) 2849–2857, doi:10.1021/la204023w.
[110] E. Morales-Narváez, A. Merkoçi, Graphene oxide as an optical biosensing platform, Adv. Mater. 24 (2012) 3298–3308, doi:10.1002/adma.201200373.
[111] R. Li, P. Georgiades, H. Cox, S. Phanphak, I.S. Roberts, T.A. Waigh, J.R. Lu, Quenched Stochastic Optical Reconstruction Microscopy (qSTORM) with Graphene Oxide, Sci. Rep. 8 (2018) 1–12, doi:10.1038/s41598-018-35297-4.
[112] F. Liu, J.Y. Choi, T.S. Seo, Biosensors and Bioelectronics Graphene oxide arrays for detecting specific DNA hybridization by fluorescence resonance energy transfer, Biosens. Bioelectron. 25 (2010) 2361–2365, doi:10.1016/j.bios.2010.02.022.
[113] C.W. Lin, K.C. Wei, S.S. Liao, C.Y. Huang, C.L. Sun, P.J. Wu, Y.J. Lu, H.W. Yang, C.C.M. Ma, A reusable magnetic graphene oxide-modified biosensor for vascular endothelial growth factor detection in cancer diagnosis, Biosens. Bioelectron. 67 (2015) 431–437, doi:10.1016/j.bios.2014.08.080.
[114] M. Li, X. Zhou, W. Ding, S. Guo, N. Wu, Biosensors and bioelectronics fluorescent aptamer-functionalized graphene oxide biosensor for label-free detection of mercury (II), Biosens. Bioelectron. 41 (2013) 889–893, doi:10.1016/j.bios.2012.09.060.
[115] V.K. Gupta, M.L. Yola, M.S. Qureshi, A.O. Solak, N. Atar, Z. Üstündağ, A novel impedimetric biosensor based on graphene oxide/gold nanoplatform for detection of DNA arrays, Sensors Actuators, B Chem 188 (2013) 1201–1211, doi:10.1016/j.snb.2013.08.034.
[116] X. Gong, Y. Bi, Y. Zhao, G. Liu, W.Y. Teoh, Graphene oxide-based electrochemical sensor: a platform for ultrasensitive detection of heavy metal ions, RSC Adv 4 (2014) 24653–24657, doi:10.1039/c4ra02247e.
[117] Z.S. Qian, X.Y. Shan, L.J. Chai, J.J. Ma, J.R. Chen, H. Feng, A universal fl uorescence sensing strategy based on biocompatible graphene quantum dots and graphene oxide for the detection of DNA †, Nanoscale 6 (11) (2014) 5671–5674, doi:10.1039/c3nr06583a.
[118] H. Jang, Y.K. Kim, H.M. Kwon, W.S. Yeo, D.E. Kim, D.H. Min, A graphene-based platform for the assay of duplex-DNA unwinding by helicase, Angew. Chemie - Int. Ed. 49 (2010) 5703–5707, doi:10.1002/anie.201001332.
[119] J.L. Chen, X.P. Yan, K. Meng, S.F. Wang, Graphene oxide based photoinduced charge transfer label-free near-infrared fluorescent biosensor for dopamine, Anal. Chem. 83 (22) (2011) 8787–8793, doi:10.1021/ac2023537.
[120] Y. Wei, L. Wang, Y. Zhang, Y. Dong, An enzyme-and label-free fluorescence aptasensor for detection of thrombin based on graphene oxide and g-quadruplex, Sensors 19 (20) (2019) 4424, doi:10.3390/s19204424.
[121] S. Pang, S. Liu, X. Su, Sensors and Actuators B : chemical An ultrasensitive sensing strategy for the detection of lead (II) ions based on the intermolecular G-quadruplex and graphene oxide, Sensors Actuators B. Chem. 208 (2015) 415–420, doi:10.1016/j.snb.2014.11.030.
[122] A. Vasilescu, S. Gáspár, M. Gheorghiu, S. David, V. Dinca, S. Peteu, Q. Wang, M. Li, R. Boukherroub, S. Szunerits, Surface Plasmon Resonance based sensing of lysozyme in serum on Micrococcus lysodeikticus-modified graphene oxide surfaces, Biosens. Bioelectron. 89 (2017) 525–531, doi:10.1016/j.bios.2016.03.040.
[123] Q. Li, Q. Wang, X. Yang, K. Wang, H. Zhang, W. Nie, High sensitivity surface plasmon resonance biosensor for detection of microRNA and small molecule based on graphene oxide-gold nanoparticles composites, Talanta 174 (2017) 521–526, doi:10.1016/j.talanta.2017.06.048.
[124] Q. Wang, B.T. Wang, Surface plasmon resonance biosensor based on graphene oxide/silver coated polymer cladding silica fiber, Sensors Actuators, B Chem 275 (2018) 332–338, doi:10.1016/j.snb.2018.08.065.
[125] N.F. Chiu, T.L. Lin, C.T. Kuo, Highly sensitive carboxyl-graphene oxide-based surface plasmon resonance immunosensor for the detection of lung cancer for cytokeratin 19 biomarker in human plasma, Sensors Actuators, B Chem 265 (2018) 264–272, doi:10.1016/j.snb.2018.03.070.
[126] I. Khalil, W.A. Yehye, N.M. Julkapli, S. Rahmati, A.A.I. Sina, W.J. Basirun, M.R. Johan, Graphene oxide and gold nanoparticle based dual platform with short DNA probe for the PCR free DNA biosensing using surface-enhanced Raman scattering, Biosens. Bioelectron. 131 (2019) 214–223, doi:10.1016/j.bios.2019.02.028.
[127] X. Fu, Y. Wang, Y. Liu, H. Liu, L. Fu, J. Wen, J. Li, P. Wei, L. Chen, A graphene oxide/gold nanoparticle-based amplification method for SERS immunoassay of cardiac troponin I, Analyst 144 (2019) 1582–1589, doi:10.1039/c8an02022a.
[128] L. Yang, S.J. Zhen, Y.F. Li, C.Z. Huang, Silver nanoparticles deposited on graphene oxide for ultrasensitive surface-enhanced Raman scattering immunoassay of cancer biomarker, Nanoscale 10 (2018) 11942–11947, doi:10.1039/c8nr02820f.
[129] A. Ali, E.Y. Hwang, J. Choo, D.W. Lim, PEGylated nanographene-mediated metallic nanoparticle clusters for surface enhanced Raman scattering-based biosensing, Analyst 143 (2018) 2604–2615, doi:10.1039/c8an00329g.
[130] C. Liu, B.J. Xu, L. Zhou, Z. Sun, H.J. Mao, J.L. Zhao, L. Zhang, X. Chen, Graphene oxide functionalized long period fiber grating for highly sensitive hemoglobin detection, Sensors Actuators, B Chem 261 (2018) 91–96, doi:10.1016/j.snb.2018.01.117.
[131] H. Fu, Y. Jiang, J. Ding, J. Zhang, M. Zhang, Y. Zhu, H. Li, Zinc oxide nanoparticle incorporated graphene oxide as sensing coating for interferometric optical microfiber for ammonia gas detection, Sensors Actuators, B Chem 254 (2018) 239–247, doi:10.1016/j.snb.2017.06.067.
[132] J. Wan, J.W. Jiang, H.S. Park, Negative Poisson's ratio in graphene oxide, Nanoscale 9 (2017) 4007–4012, doi:10.1039/c6nr08657h.
[133] H. Belyadi, E. Fathi, F. Belyadi, Rock mechanical properties and in situ stresses, Hydraul. Fract. Unconv. Reserv. (2019) 215–231, doi:10.1016/b978-0-12-817665-8.00013-8.
[134] W. Chen, X. Gui, L. Yang, H. Zhu, Z. Tang, Wrinkling of two-dimensional materials: methods, properties and applications, Nanoscale Horizons 4 (2019) 291–320, doi:10.1039/c8nh00112j.
[135] I. Tiwari, M. Singh, C.M. Pandey, G. Sumana, RSC Advances Electrochemical detection of a pathogenic Escherichia coli speci fi c DNA sequence based on a graphene oxide – chitosan composite decorated with nickel ferrite nanoparticles †, RSC Adv 5 (2015) 67115–67124, doi:10.1039/C5RA07298K.
[136] Y. Luo, X. Sun, Synthesis of Au nanoparticles decorated graphene oxide nanosheets : noncovalent functionalization by TWEEN 20 in situ reduction of aqueous chloroaurate ions for hydrazine detection and catalytic reduction of, J. Hazard. Mater. 197 (2011) 320–326, doi:10.1016/j.jhazmat.2011.09.092.
[137] F. He, J. Fan, D. Ma, L. Zhang, C. Leung, H.L. Chan, The attachment of Fe 3 O 4 nanoparticles to graphene oxide by covalent bonding, Carbon N. Y. 48 (2010) 3139–3144, doi:10.1016/j.carbon.2010.04.052.
[138] T. Wang, S. Zhang, C. Mao, J. Song, H. Niu, B. Jin, Y. Tian, Biosensors and Bioelectronics Enhanced electrochemiluminescence of CdSe quantum dots composited with graphene oxide and chitosan for sensitive sensor, Biosens. Bioelectron. 31 (2012) 369–375, doi:10.1016/j.bios.2011.10.048.
[139] Y. Zhang, Y. Wang, J. Jia, J. Wang, Nonenzymatic glucose sensor based on graphene oxide and electrospun NiO nanofibers, Sensors Actuators, B Chem 171–172 (2012) 580–587, doi:10.1016/j.snb.2012.05.037.
[140] M.A. Ali, W. Hong, S. Oren, Q. Wang, Y. Wang, H. Jiang, L. Dong, Tunable bioelectrodes with wrinkled-ridged graphene oxide surfaces for electrochemical nitrate sensors, RSC Adv 6 (2016) 67184–67195, doi:10.1039/c6ra09621b.
[141] A. Prasad, A. Chaichi, A. Mahigir, S.P. Sahu, D. Ganta, G. Veronis, M.R. Gartia, Ripple mediated surface enhanced Raman spectroscopy on graphene, Carbon N. Y. 157 (2020) 525–536, doi:10.1016/j.carbon.2019.09.078.
[142] K.J. Lee, D. Kim, B.C. Jang, D.J. Kim, H. Park, D.Y. Jung, W. Hong, T.K. Kim, Y.K. Choi, S.Y. Choi, Multilayer graphene with a rippled structure as a spacer for improving plasmonic coupling, Adv. Funct. Mater. 26 (2016) 5093–5101, doi:10.1002/adfm.201601850.
[143] A.K. Sood, I. Lund, Y.R. Puri, H. Efstathiadis, P. Haldar, N.K. Dhar, J. Lewis, M. Dubey, E. Zakar, P. Wijewarnasuriya, D.L. Polla, M. Fritze, Review of

graphene technology and its applications for electronic devices, Graphene - New Trends Dev. (2015), doi:10.5772/61316.
[144] T. Ando, The electronic properties of graphene and carbon nanotubes, NPG asia materials 1 (1) (2009) 17–21, doi:10.1038/asiamat.2009.1.
[145] L. Tapasztó, T. Dumitrica, S.J. Kim, P. Nemes-Incze, C. Hwang, L.P. Biró, Breakdown of continuum mechanics for nanometre-wavelength rippling of graphene, Nat. Phys. 8 (2012) 739–742, doi:10.1038/nphys2389.
[146] K.S. Novoselov, A.H. Castro Neto, Two-dimensional crystals-based heterostructures: materials with tailored properties, Phys. Scr. (2012) 014006, doi:10.1088/0031-8949/2012/T146/014006.
[147] P. Mardling, A. Alderson, N. Jordan-Mahy, C.L. Le Maitre, The use of auxetic materials in tissue engineering, Biomater. Sci. 8 (2020) 2074–2083, doi:10.1039/c9bm01928f.